Research paper

Metallo-β-lactamase inhibitors by bioisosteric replacement: Preparation, activity and binding

CrossMark

Susann Skagseth [a, 1], Sundus Akhter [b, 1], Marianne H. Paulsen [b, 2], Zeeshan Muhammad [b], Silje Lauksund [c], Ørjan Samuelsen [c, d], Hanna-Kirsti S. Leiros [a, **], Annette Bayer [b, *]

[a] The Norwegian Structural Biology Centre (NorStruct), Department of Chemistry, Faculty of Science and Technology, UiT The Arctic University of Norway, N-9037 Tromsø, Norway
[b] Department of Chemistry, Faculty of Science and Technology, UiT The Arctic University of Norway, N-9037 Tromsø, Norway
[c] Norwegian National Advisory Unit on Detection of Antimicrobial Resistance, Department of Microbiology and Infection Control, University Hospital of North Norway, N-9038 Tromsø, Norway
[d] Department of Pharmacy, UiT The Arctic University of Norway, N-9037 Tromsø, Norway

ARTICLE INFO

ABSTRACT

Bacterial resistance is compromising the use of β-lactam antibiotics including carbapenems. The main resistance mechanism against β-lactams is hydrolysis of the β-lactam ring mediated by serine- or metallo-β-lactamases (MBLs). Although several inhibitors of MBLs have been reported, none has been developed into a clinically useful inhibitor. Mercaptocarboxylic acids are among the most prominent scaffolds reported as MBL inhibitors. In this study, the carboxylate group of mercaptocarboxylic acids was replaced with bioisosteric groups like phosphonate esters, phosphonic acids and NH-tetrazoles. The influence of the replacement on the bioactivity and inhibitor binding was evaluated. A series of bio-isosteres of previously reported inhibitors was synthesized and evaluated against the MBLs VIM-2, NDM-1 and GIM-1. The most active inhibitors combined a mercapto group and a phosphonate ester or acid, with two/three carbon chains connecting a phenyl group. Surprisingly, also compounds containing thioacetate groups instead of thiols showed low IC_{50} values. High-resolution crystal structures of three inhibitors in complex with VIM-2 revealed hydrophobic interactions for the diethyl groups in the phosphonate ester (inhibitor **2b**), the mercapto bridging the two active site zinc ions, and tight stacking of the benzene ring to the inhibitor between Phe62, Tyr67, Arg228 and His263. The inhibitors show reduced enzyme activity in *Escherichia coli* cells harboring MBL. The obtained results will be useful for further structural guided design of MBL inhibitors.

© 2017 Elsevier Masson SAS. All rights reserved.

1. Introduction

Antibiotics are essential for modern medicine and as antibiotics are now becoming increasingly ineffective, effective treatment of an ever-increasing range of infections is threatened [1,2]. As defence mechanism against β-lactam antibiotics, bacteria are able to produce β-lactamases that hydrolyze and inactivates the antibiotic [3,4]. β-Lactamases are grouped into two super families, the serine dependent β-lactamases (SBLs; Amber class A, C, and D) and metallo-β-lactamases (MBLs; Amber class B) [5,6]. The MBLs are classified into three subclasses (B1, B2 and B3), with the majority of nosocomial MBLs belonging to the B1 subclass. This includes variants of the Verona integron-encoded metallo-β-lactamase (VIM), the New Delhi metallo-β-lactamase (NDM) [7], and the German Imipenemase (GIM). The active site of the B1 MBLs is generally well preserved despite large variation in the second shell interacting residues. The active site holds two cationic zinc ions (Zn1, Zn2), as a metal co-factor of enzyme activity, which are coordinated by H116, H118 and H196 (Zn1) and D120, C221 and H263 (Zn2) [8,9]. Here and throughout the paper, the standard numbering scheme for class B β-lactamases is used [10]. In general, the sequence identity among the class B1 MBLs is low. For the enzymes used in this study, the sequence identity is 32% between VIM-2 and NDM-1, 28% for VIM-2 versus GIM-1 and 24% between NDM-1 and GIM-1 (Fig. S1 in

SI).

The MBLs hydrolyze a broad spectrum of β-lactam antibiotics [3,8,11,12] including the last resort antibiotics; the carbapenems. In addition, genes encoding certain MBLs are associated with mobile genetic elements and can spread across different types of Gram-negative bacteria [7,11]. Inhibitors of SBLs are available clinically [13], including the broad spectrum inhibitor avibactam [14]. Unfortunately, all SBL inhibitors lack activity against MBLs [15]. Although the search for MBL inhibitors started from mid 1990s, and a wide variety of scaffolds has been reported [16—18], clinically useful MBL inhibitors remain an elusive goal.

In this study we decided to explore the use of thiol-based compounds as one of our strategies to gain increased knowledge on MBL inhibitors. Thiols have the potential to coordinate the zinc ions in the MBL active site, due to the thiophilic nature of zinc, and thereby preventing β-lactam hydrolysis. Some mercaptocarboxylic acids have been evaluated successfully against several MBLs [19—32], making this class of compounds an interesting starting point for further investigations. Our focus was to elucidate the effect of replacement of the carboxylate group in the promising mercaptocarboxylic acid scaffold with bioisosters on the bioactivity and enzyme-inhibitor binding. Bioisosteric replacement is a concept in medicinal chemistry to rationally improve the activity or physicochemical properties of biologically active compounds [33]. A structural element of a biological active compound is replaced with a substitute that maintain some of the properties of the parent structure, e.g. inhibitor binding to a biological target, while others are changed, e.g. lipophilicity or steric size. Typical bioisosters of carboxylic acids include among others phosphonates, NH-tetrazoles and sulphonamides [34].

The target structures 2—4 (Scheme 1) were envisioned by substitution of the carboxylate group of the known mercaptocarboxylic acid inhibitor 1 [25,35] with bioisosteric groups like phosphonate esters, phosphonic acids or NH-tetrazoles, respectively. The carbon chain of the alkylphenyl substituent was varied (n = 2—4; Scheme 1) with the goal to evaluate the effect of chain length on hydrophobicity and bioactivity. The compounds and relevant intermediates from the synthetic pathway were simultaneous evaluated against the three MBLs VIM-2, NDM-1 and GIM-1 with the goal to find MBL inhibitors able to act on several different MBL subfamilies. For each target we have determined the IC_{50} value through enzyme inhibition assays and the effect of the inhibitors in whole cell E. coli assays with VIM-2, GIM-1 or NDM-1. Some inhibitors were also tested in a synergy assay with two or three clinical isolates from Pseudomonas aeruginosa, Klebsiella pneumoniae or Escherichia coli. The enzyme-inhibitor complexes of the best inhibitors were further evaluated by X-ray analysis and the impact from second shell interacting residues on ligand binding were examined.

2. Results and discussion

2.1. Chemistry

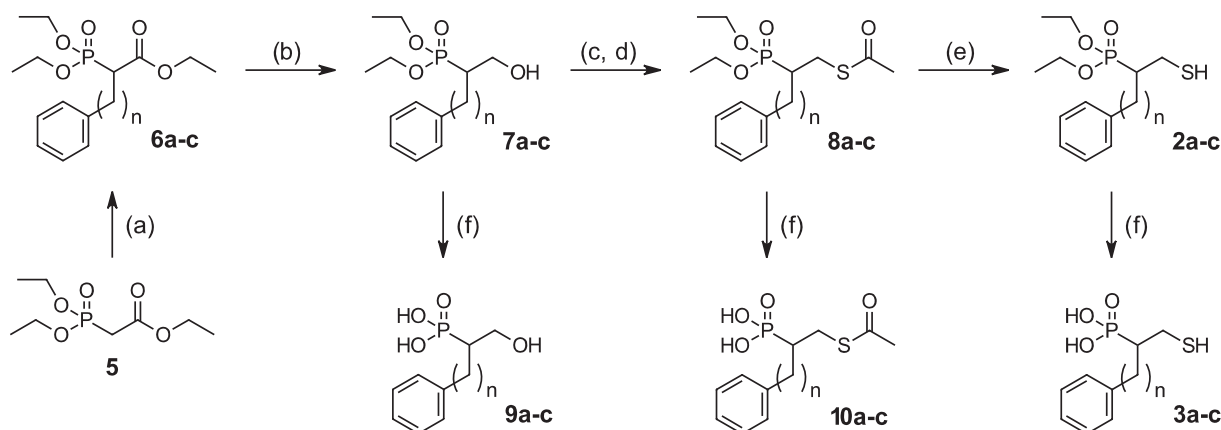For the purpose of this work, all compounds (Schemes 2 and 3)
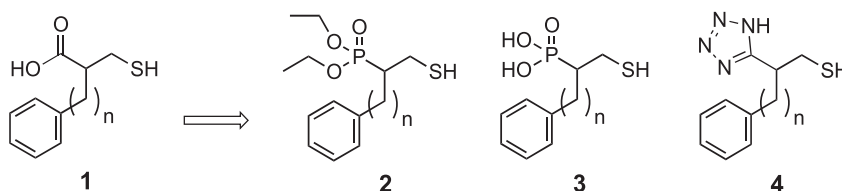
were prepared as racemic mixtures. Phosphonate ester 2a—c and phosphonic acid 3a—c analogues with differing chain lengths (n = 2—4) were prepared according to the synthetic strategy presented in Scheme 2. Triethyl phosphonoacetate 5 was alkylated using potassium tert-butoxide (KOtBu) as base to afford the mono-alkylated acetates 6a—c in moderate yields (45—73%). Chemoselective reduction of the ester in presence of the phosphonate was obtained with lithium borohydrid to provide the corresponding alcohols 7a—c. Subsequent mesylation followed by substitution with potassium thioacetate gave the thioacetates 8a—c. Several methods for deprotection of the thioacetates were evaluated [36—38]. Best results were obtained by treatment with sodium methylthiolate (NaSMe) providing the free thiols 2a—c in good yields (74—77%) and purity (>95% by HPLC). The phosphonates ester analogues 2, 7 and 8 were purified by normal-phase flash column chromatography to >95% purity as determined by HPLC analysis. The diethyl phosphonates 2, 7 and 8 were transferred to the corresponding phosphonic acid derivatives 3, 9 and 10, respectively, by treatment with trimethylsilyl bromide (TMSBr) followed by a MeOH quench. Purification of the phosphonic acid analogues 3, 9 and 10 could be achieved by washing with EtOAc/pentane to provide the target compounds with moderate to good yields and purity >95% as determined by HPLC analysis.

The NH-tetrazole analogues 4, 15 and 16 were prepared as shown in Scheme 3 α-Substituted acrylonitriles 13a and 13b with varying chain lengths (n = 1, 3) were prepared by a procedure based on the work of Baraldi et al. [39]. Microwave promoted reaction of the acrylonitriles with trimethylsilyl azide with dibutyltinoxide as catalyst (20 mol%) [40] gave the corresponding NH-tetrazoles 14a and 14b (74—78% yield), which proved to be excellent Michael acceptors. The addition of potassium thioacetate resulted in the tetrazolyl thioacetates 15a and 15b in good yields (>95%), while the addition of cyclohexanethiol gave 16 (93% yield). Deprotection of the thioacetates by treatment with sodium methylthiolate (NaSMe) provided the free thiol 4 in moderate yield (74%) and purity >96% as determined by HPLC analysis.

2.2. Characterization of inhibitor properties against VIM-2, GIM-1 and NDM-1

The inhibitory activities of the mercaptocarboxylic acid 1c [25] and bioisosters 2a—c, 3a—c and 4, as well as several intermediates from the synthesis (7—10 a—c, 15a, 15b and 16) were determined by the half maximal inhibitory concentration (IC_{50}) values (Table 1). For VIM-2 and GIM-1, the IC_{50} values were measured using nitrocefin as a reporter substrate, while IC_{50} values for NDM-1 were measured with imipenem as reporter substrate. Nitrocefin is hydrolyzed by NDM-1 with a high catalytic efficiency and unsuitable as a reporter substrate for NDM-1 [41]. The influence of dimethyl sufoxide (DMSO) on the enzyme activity was investigated in the assay, and a concentration of 2.5% DMSO was tolerated without influencing the enzyme activity (data not shown). The IC_{50} values were determined by measuring the initial rate of the reactions with inhibitors at different concentration in a 2-fold dilution series, and were fitted to a dose-response curve (IC_{50}

Scheme 1. Design of new MBL inhibitors through bioisosteric substitution of the carboxylate group.

Scheme 2. Synthesis of phosphonate and phosphonic acid containing thiol-based inhibitors. Reagents and conditions: **a**: n = 2; **b**: n = 3; **c**: n = 4; (a) R—Br, KOtBu, DMF, 0 °C, **6a**: 62%, **6b**: 73%, **6c**: 45%; (b) LiBH$_4$, THF, MW 80 °C for 10 min, **7a**: 60%, **7b**: 95%, **7c**: 56%; (c) MsCl, Et$_3$N, DMAP, CH$_2$Cl$_2$, rt; (d) KSAc, DMF, rt.; **8a**: 54%, **8b**: 34%, **8c**: 71% over two steps; (e) NaSMe, MeOH, −20 °C, **2a**: 30%, **2b**: 74%, **2c**: 77%; (f) TMSBr, CH$_2$Cl$_2$, then MeOH, rt., **3a**: 96%, **3b**: 90%, **3c**: 98%, **9a**: 76%, **9b**: 61%, **9c**: 55%, **10a**: 91%, **10b**: 71%, **10c**: 65%.
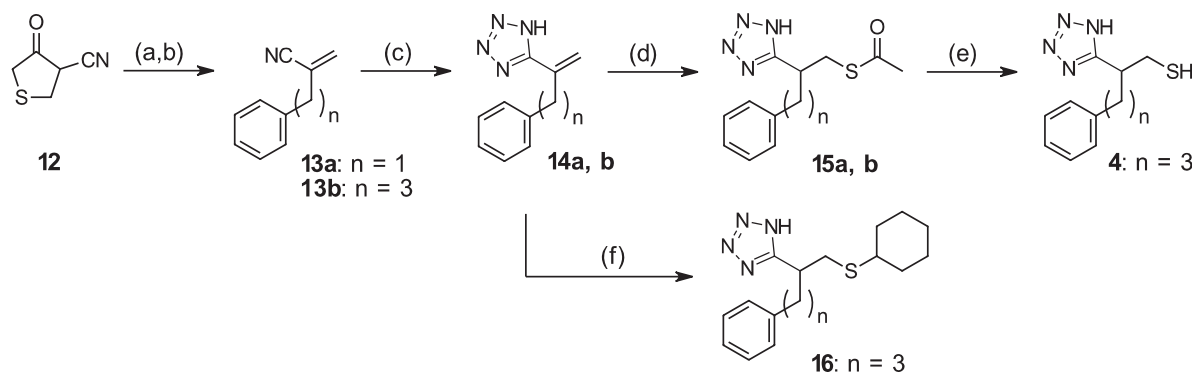
Scheme 3. . Synthesis of NH-tetrazole containing thiol based inhibitors. Reagents and conditions: **a**: n = 1; **b**: n = 3; (a) R—Br, K$_2$CO$_3$, acetone, reflux; (b) 5% aq. NaOH, **13a**: 51%, **13b**: 21%; (c) TMSN$_3$, n-Bu$_2$SnO (20 mol%), 1,4-dioxane, MW 150 °C for 50 min, **14a**: 78%, **14b**: 74%; (d) HSAc, DMF, 60 °C, **15a**: 95%, **15b**: 98%; (e) NaSMe, MeOH, −20 °C, **4**: 74%; (f) cyclohexylthiol, DMF, 60 °C, **16**: 93%.

curves are given in Fig. S2—S4 in SI).

In order to validate our assay, the IC$_{50}$ of the previously reported VIM-2 inhibitor **1c** [25] was measured against VIM-2. We obtained an IC$_{50}$ of 2.9 μM, which is in the same range as the reported value of 1.1 μM (Table 1). The difference in IC$_{50}$ values is most likely due to different assay buffers and protein constructs. The new compounds showed IC$_{50}$ values ranging from 0.38 to 133 μM with VIM-2, 0.18 to >5000 μM with GIM-1 and 1.8—144 μM with NDM-1 (Table 1 and S1 in SI). The synthetic intermediates **7**—**9 a**—**c**, **15a** and **15b** did not have inhibitory activity (IC$_{50}$ > 10 μM, see Table S1 in SI) against any of the MBLs. Compounds **2a**—**c**, **3a**—**c**, **4**, **10a**—**c** and **16** showed activity at varying levels. In general, the inhibitors showed better IC$_{50}$ values towards VIM-2 compared to GIM-1 and NDM-1, with the exception of inhibitor **2a**, which had a ~five times lower IC$_{50}$ for GIM-1 (0.18 μM) compared to VIM-2 (0.89 μM).
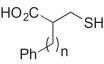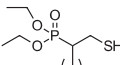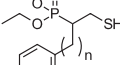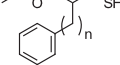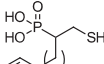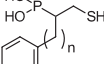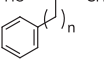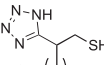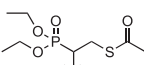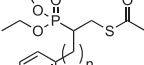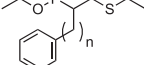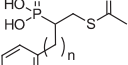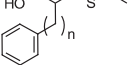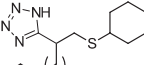
Inhibitors **2a** and **2b** showed IC$_{50}$ values ranging from 0.18 to 2.2 μM for all three MBLs. The IC$_{50}$s were within the same range for VIM-2 and GIM-1, and slightly increased for NDM-1 (1.8—2.2 μM). Inhibitor **2c** precipitated from the buffer solution and was not evaluated further. The results indicate that for the mercapto-phosphonates **2**, lengthening the side chain from two (**2a**) to three methylene groups (**2b**), did not have a great effect on the activity.

While the mercaptophosponate esters **2** showed highest activity against GIM-1, the mercapto- and thioacetate phosphonic acids, **3** and **10**, were more active towards VIM-2 and NDM-1 than GIM-1. The IC$_{50}$ values for thioacetate phosphonic acids **10a**—**c** ranged

from 1.8 to 4.7 μM, and from 2.5 to 6.6 μM for VIM-2 and NDM-1, respectively. With GIM-1 the inhibitors **10a**—**c** showed slightly higher IC$_{50}$ values of 12—26 μM. The same trend was seen with the mercaptophosphonic acids **3a** and **c**, where the IC$_{50}$ values for VIM-2 and NDM-1 were in the same range (7.8 and 8.6 μM with VIM-2 and 5.9 and 8.5 μM with NDM-1, respectively), while the values for GIM-1 were 2—4 fold higher (23 and 16 μM, respectively). A possible explanation for this might be that GIM-1 has a narrower active site compared to other MBLs due to the aromatic side chains Trp228 and Tyr233 [42]. However, this does not explain the low IC$_{50}$ values for inhibitors **2a** and **2b**.

Substituting the carboxylic acid of compound **1** with a NH-tet-razole (**4**) had a deteriorating effect on the inhibitory activity, while substitution with phosphonate esters and phosphonic acids groups led to similar (**2** and **10**) or improved (**3**) activity. Comparing the inactive alcohols **7** and **9** with the corresponding active thiols and thioacetates **2**, **3** and **10** illustrates the importance of the sulfur atom on the β-carbon for the inhibitor activity. However, activity seem to depend on a subtle combination of the sulfur atom and a carboxylic acid bioisoster as revealed when comparing the mer-capto and thioacetate substituted phosphonate esters and phos-phonic acids **2**, **3**, **8** and **10**. The mercapto substituted phosphonate esters **3** were the overall most active inhibitors, while the thio-acetate substituted phosphonate esters **8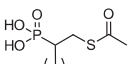** showed the lowest ac-tivity of all four. Surprisingly, the same trend was not observed for the pair of phosphonic acids **2** and **10**. Here, the thiol **2** and the

Table 1
Evaluation of compound **1c** and bioisosteres thereof as inhibitors of VIM-2, GIM-1 or NDM-1 measured as inhibition concentrations (IC$_{50}$) against purified enzyme and percent inhibition in *E. coli* SNO3 bacterial whole cell experiments.

Compound		VIM-2[a]		GIM-1[a]		NDM-1[b]	
		IC$_{50}$ (μM)	% inhib	IC$_{50}$ (μM)	% inhib	IC$_{50}$ (μM)	% inhib
(structure)	**1c** (n = 4)	2.9 (1.1)[c]		–	–	56	–
(structure)	**2a** (n = 2)	0.89	78	0.18	64	2.2	33
	2b (n = 3)	0.38	79	0.31	48	1.8	62
	2c (n = 4)	p[d]	p[d]	p[d]	p[d]	p[d]	p[d]
(structure)	**3a** (n = 2)	7.8	92	23	37	5.9	42
	3b (n = 3)	33.2	95	28	46	7.1	45
	3c (n = 4)	8.6	94	16	31	8.5	42
(structure)	**4** (n = 3)	28	67	68	25	12	16
(structure)	**8a** (n = 2)	133	17	18	25	nh[e]	i[f]
	8b (n = 3)	34	14	26	21	nh[e]	i[f]
	8c (n = 4)	20	12	13	25	nh[e]	i[f]
(structure)	**10a** (n = 2)	2.3	94	12	40	2.9	39
	10b (n = 3)	4.7	95	26	37	6.6	38
	10c (n = 4)	1.8	97	20	50	2.5	37
(structure)	**16** (n = 3)	5	73	36	8	10	i[f]

[a] Reporter substrate used was nitrocefin (NCF).
[b] Reporter substrate used was imipenem (IPM).
[c] Values in parentheses as reported by Jin et al. [25].
[d] p = precipitated in buffer and was not tested.
[e] nh = no hydrolysis.
[f] i = inactive.

thioacetate **10** inhibited the MBLs at the same level, which may indicate that the interaction of the phosphonic acid with the enzyme is more important for the activity than the interaction with the thiol. This interpretation would be in agreement with the previously reported observation that a mercaptophosphonic acid coordinated the MBL CphA by the two oxygen atoms of the phosphonic acid and not by the sulfur atom of the thiol [43].

The most active inhibitors showed activity in the low micromolar to high nanomolar range for the racemic mixtures. In two recent studies, pure stereoisomers of the mercaptocarboxylic acids captopril [19] and bisthiazolidine [21] were found to display 10–100 times differences in inhibitory activity between different stereoisomers. This will most likely be the case for the compounds prepared in this work, and for future work this can be pursued. A large variation in inhibitory activity towards three B1 MBLs was observed, which indicates that these inhibitors do not fulfill the requirements for a broad-spectrum MBL inhibitor.

2.3. Evaluation of inhibitors in bacterial cell assays

To investigate if the inhibitors were active against MBLs in bacterial cells, two different assays were used. Initially, the inhibitors were tested in a whole cell assay using *E. coli* SNO3 cells with *bla*$_{VIM-2}$, *bla*$_{GIM-1}$ or *bla*$_{NDM-1}$ in pET26b(+) (Table 1). The inhibitory activity were measured as percent inhibition calculated by measuring the slope of the initial hydrolysis of the reporter substrates for up to 60 min, and the slope of a control without inhibitor present, according to equation (1).

The percent inhibition for the most active compounds is shown in Table 1. High percent inhibition (>70%) was observed for several compounds, which indicates that the compounds pass the bacterial cell membrane of *E. coli*. The highest percent inhibition was observed for inhibitors **3a**–**c** and **10 a**–**c** in *E. coli* with VIM-2, with 92–95% and 94–97% inhibition, respectively. These results are in agreement with the low IC$_{50}$ values (1.8–8.6 and 33 μM). The inhibitory activities of **3a**–**c** and **10a**–**c** were less pronounced with GIM-1 and NDM-1 resulting in an inhibition of around 30–50%, although the IC$_{50}$ values against NDM-1 were in the same range as against VIM-2.

The inhibitors **2a** and **2b**, showing lowest IC$_{50}$ values, showed 78% and 79% inhibition with VIM-2, respectively. While the percent inhibition of inhibitor **2a** and **2b** were 64% and 48% for GIM-1 and

33% and 62% for NDM-1, respectively. The phosphonate esters **2** were found to be more hydrophobic at pH 7.1 (clogD = 3.4—3.8), which is the pH of the buffer medium, compared to the phosphonic acids **3** and **10** (clogD = −0.9—0.1), which probably results in poorer passive permeability [44] of the former explaining the lower % inhibition observed for these compounds. For NDM-1, inhibitor **2b** was the best inhibitor in terms of the lowest IC$_{50}$ and highest effect in the cell-based screening assay. Modification of **2** to alter the physicochemical properties may by a direction for further inhibitor improvement.

Additionally, the inhibitors were tested for synergistic activity with meropenem against MBL-producing clinical strains, and effect from the inhibitors alone on the bacterial growth. The results are given in Table S2 in the SI. Disappointingly, synergy testing of the inhibitors with meropenem using bacterial strains from *P. aeruginosa* or *K. pneumoniae* did not show a lowering of the MIC. However, promising results were observed when **3b** and **10b** were tested against an *E. coli* strain with VIM-29. In these experiments, the MIC was lowered from 8 to 32 mg/L with only meropenem to 1 mg/L in presence of inhibitors (Table S2 in SI). Since VIM-2 has 90% sequence identity to VIM-29 it is likely to believe that VIM-2 could also be inhibited in a similar assay. In addition, the tested compounds were not toxic at high concentrations (>500 μM) to the three clinical cell lines included in this study (Table S2 in SI).

2.4. Crystal structure complexes of VIM-2 with *2b*, *10b* and *10c*

To better understand the effects of bioisosteric substitution and to address the question of the coordinating properties of the phosponic acid group compared to the thiol, we attempted to obtain complex structures of the new inhibitors. Initial attempts to soak native crystals were found unsuccessful, whereas our new protocol for a DMSO free co-crystallization method [45] was successful for inhibitors **2b, 10b** and **10c**. Several more inhibitors were included in the experiment without providing satisfactory complexes. All the new VIM-2 complex structures have two protein molecules in the asymmetric unit, a αβ/βα fold with mobile loops adjacent to the active site, and there are two zinc ions in the active site, Zn1 bound to His116, His118 and His196 and Zn2 coordinated by Asp120, Cys221 and His263. For all structures, the interactions in the best-defined protein chain will be described, and only discrepancies for other chain will be mentioned.

The VIM-2_**2b** complex was the best-defined complex to 1.55 Å (Table 2) and this complex was used to investigate the two different enantiomers. Herein, the (*S*)-form of the inhibitor **2b** did not fit into the observed polder omit map (Fig. 1A), whereas for the (*R*)-form (Fig. 1B), the substituents at the stereogenic center are all defined within the polder omit map. Therefore, we anticipate that VIM-2 is selectively binding the (*R*)-enantiomer of **2b**, since the CH$_2$-SH group, the CH$_2$-CH$_2$ chain and the phosphonate ester are defined inside both the polder omit and the final 2Fo-Fc map (Fig. 1B, C). The three-dimensional arrangement of substituents on the stereogenic center of (*R*)-**2b** (Fig. 2) is in agreement with the reported complex of VIM-2_**1b** [35] selectively bound to (*S*)-**1b**. Note that the difference in naming of the stereoisomers ((*S*)-**1b** versus (*R*)-**2b**) relates to differences in priority according to the Khan-Ingold-Prelog rules (for **1b**: CH$_2$SH > CO$_2$H while for **2b**: P(O)(OH)$_2$ > CH$_2$SH) not to inversion of the stereocenter. For both VIM-2_**10b** and **10c** structures, the (*R*)-configuration fits best in the polder omit and 2Fo-Fc maps (Fig. 1D—I), but less convincing than for the highest resolved VIM-2_**2b** complex (Fig. 1A—C). This indicates that for the structurally related compounds of this study the three-dimensional arrangement corresponding to the (*R*)-configuration probably leads to inhibitors with improved binding and inhibition properties.

Table 2
X-ray data collection and crystallographic refinement statistics for VIM-2 complexes of **2b**, **10b** and **10c**. Values in parenthesis are for the highest resolution shell.

	VIM-2_**2b**	VIM-2_**10b**	VIM-2_**10c**
PDB entry	5MM9	5NHZ	5NI0
X-ray source	ID29, ESRF	ID29, ESRF	ID29, ESRF
Data collection statistics			
Space group	C2	P2$_1$2$_1$2$_1$	P2$_1$2$_1$2$_1$
Unit cell (Å)			
a	101.11	45.78	45.72
b	79.07	90.87	91.07
c	67.47	124.08	122.92
β (°)	130.3		
Resolution (Å)	24.94—1.55	24.75—1.85	24.77—1.67
	(1.61—1.55)	(1.92—1.85)	(1.73—1.67)
Wavelength (Å)	0.97 625	0.97 625	0.97 625
No. unique reflections	54 949 (5447)	45 000 (4421)	56 573 (5666)
Multiplicity	2.0 (1.9)	6.5 (6.7)	6.4 (6.3)
Completeness (%)	93.58 (93.51)	99.93 (99.98)	94.12 (92.38)
Mean (<I>/<σ$_I$>)	8.16 (1.92)	14.60 (2.30)	10.80 (1.61)
R-merge[a]	0.064 (0.417)	0.073 (0.791)	0.102 (0.925)
CC $_{1/2}$	0.995 (0.679)	0.999 (0.785)	0.997 (0.634)
Resolution (Å)	24.94—1.55	24.75—1.85	24.77—1.67
	(1.61—1.55)	(1.92—1.85)	(1.73—1.67)
Wavelength (Å)	0.97 625	0.97 625	0.97 625
No. unique reflections	54 949 (5447)	45 000(4421)	56 573 (5666)
Multiplicity	2.0 (1.9)	6.5 (6.7)	6.4 (6.3)
Completeness (%)	93.58 (93.51)	99.93 (99.98)	94.12 (92.38)
Mean (<I>/<σ$_I$>)	8.16 (1.92)	14.60 (2.30)	10.80 (1.61)
R-merge[a]	0.064 (0.417)	0.073 (0.791)	0.102 (0.925)
CC $_{1/2}$	0.995 (0.679)	0.999 (0.785)	0.997 (0.634)
Wilson B-factor (Å^2)	14.84	27.24	20.49
Refinement statistics			
Resolution (Å)	24.94—1.55	25—1.85	25—1.67
R-factor (all reflections)	0.1575	0.1662	0.1778
R-free[b]	0.2006	0.2039	0.2140
RMSD bond lengths (Å)	0.011	0.013	0.011
RMSD bond angles (°)	1.31	1.32	1.32
Ramachandran favored (%)	98.0	97.0	97.0
Ramachandran outliers (%)	0.46	0.47	0.95
Clashscore	5.50	3.00	5.62
Average B-factor (Å^2)			
All atoms	20.8	36.5	27.4
Chain A/B	20.6/20.6	32.6/37.2	25.3/26.18
Solvent	34.0	47.9	37.0
Ligand A/B	40.3/32.8	47.5/58.5	63.04/64.24
Mean occupancy			
Zn1 A/B	0.9/0.9	1.0/1.0	1.0/1.0
Zn2 A/B	0.75/1.0	0.6/0.7	0.7/0.5
Ligand A/B	1.0/0.9	0.7/0.8	0.9/0.9

In the VIM-2_**2b** crystal structure there are hydrogen bonds from the OAE atom of the P=O double bond in compound **2b** to the Asn233 sidechain (d(OAE$_{ligand}$ … ND2$_{N233}$) = 2.84 Å) and from the SH group to both zinc ions (d(S$_{ligand}$ … Zn1/Zn2) = 2.30/2.30 Å). Further, the benzene ring of compound **2b** is sandwiched between Arg228 and Tyr67, making T-shaped π-π stacking interactions with Tyr67 and cation-π interactions with the positively charged Arg288 in a parallel manner. The benzene ring is also in a T-shaped stacking conformation with His263. Additionally, the ethyl groups of the phosphonate ester make hydrophobic interactions with Phe61, Tyr67, Trp87, and CA and CB carbon atoms of Asp119 (Fig. 3A). These two ethyl groups are absent in the corresponding phosphonic acids **3**, which display higher IC$_{50}$ values (7.8—33.2 μM) towards VIM-2 than the phosphonate esters **2** (0.38—1.7 μM) (Table 1), indicating that the phosphonic acid group is not involved in corresponding favorable interactions.

Comparison of the VIM-2_**2b** structure with the previously reported complex of VIM-2_**1b** [35] (Fig. 2D) showed that the sulfur atom of thiol **2b** is bridging the zinc(II) atoms of VIM-2 resembling the earlier reported complex of VIM-2_**1b** and numerous other

A) VIM-2_**2b**, Polder map
S-form

B) VIM-2_**2b**, Polder map
R-form

C) VIM-2_**2b**, 2Fo-Fc map

D) VIM-2_**10b**, Polder map
S-form

E) VIM-2_**10b**, Polder map
R-form

F) VIM-2_**10b**, 2Fo-Fc map

G) VIM-2_**10c**, Polder map
S-form

H) VIM-2_**10c**, Polder map
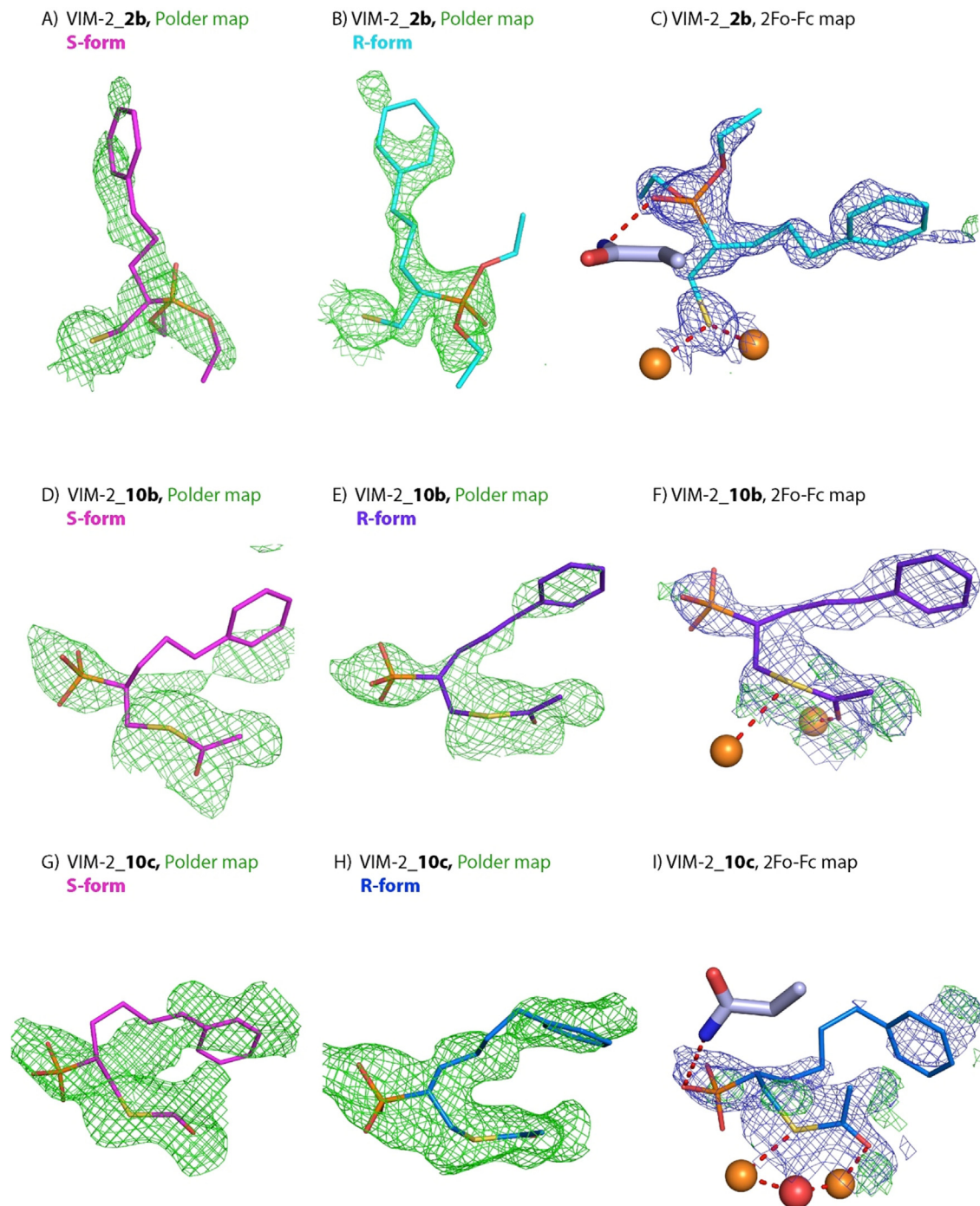**R-form**

I) VIM-2_**10c**, 2Fo-Fc map

Fig. 1. Observed electron density maps for the new inhibitors with polder omit maps depicted at 2.5σ (green), 2Fo-Fc maps at 1.0 σ (blue) and Fourier difference maps (Fo-Fc) at 4.0 σ (green) and −4.0 σ (red). The polder omit maps for VIM-2 with the inhibitors **2b**, **10b** and **10c** in (S)-form (left panels), (R)-form (middle panels) and the final 2Fo-Fc map (right panels) are displayed. The zinc ions (orange) and adjacent water (red) are shown, and hydrogen bonds are shown as red dashed lines. (For interpretation of the references to colour in this figure legend, the reader is referred to the web version of this article.)

thiol-B1 MBL complex structures [19,23,28,35,46—49]. Also, the propylphenyl chains of both **1b** and **2b** occupy the same region in VIM-2. Still there is a T-shaped stacking for Phe61 and phenyl in our new **2b** complex, and a face-to-face more parallel π-π stacking for **1b** (PDB ID: 2YZ3) [35]. Both the carboxyl group of **1b** and the phosphonate P=O of **2b** are forming hydrogen bonds with the ND2 atom in the side chain of Asn233. The slightly different orientations of the inhibitors **1b** and **2b** may be attributed to the hydrophobic interactions of the two ethyl groups of **2b** with residues Phe61,

Tyr67, Trp87, and CA and CB carbon atoms in the Asp119 (Fig. 3A).

The resolution of the VIM-2_**10b** structure is 1.85 Å, and this inhibitor was refined in the (R)-form since this fitted best in the observed electron density maps (Fig. 1D, E). In the final electron density maps the orientation of the thioacetate group is described adequately but the width of the electron density is indicating flexibility and there is positive election in the Fo-Fc map. This additional density could be ascribed to the hydroxyl ion between Zn1 and Zn2, but this could not be modeled and is thus left out in
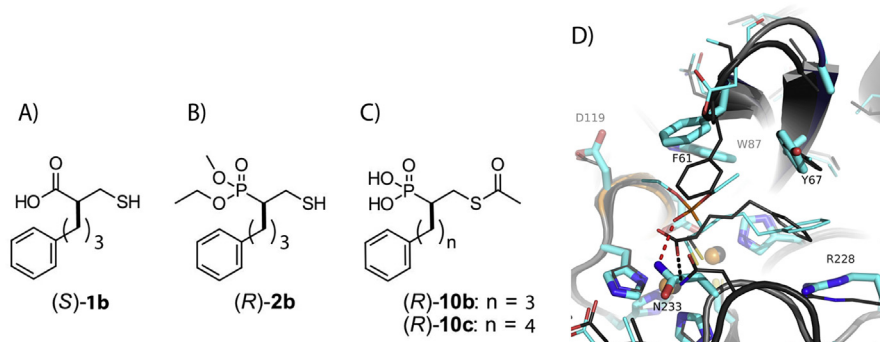
Fig. 2. A-C) Stereochemical view of the enantiomeric form of **1b**, **2b**, **10b** and **10c** coordinated and bound to VIM-2. D) Overlay of VIM-2_**2b** (cyan) and previously reported VIM-2_**1b** [35] (grey). (For interpretation of the references to colour in this figure legend, the reader is referred to the web version of this article.)

the final structure. Further, there is additional unmodeled density in elongation of the methyl group of the thioacetate of **10b**. The complex of VIM-2_**10c** is very similar to VIM-2_**10b**. Still, for the VIM-2_**10c** structure, a hydroxyl ion bridging Zn1 and Zn2 in both chain A and chain B could be modeled, but the methylene chain is not well defined in the electron density and displays high B-factors (Table 2, Fig. 1H and I).

From the VIM-2_**10b** and **10c** complex structures, it is clear that the sulfur atom of the thioacetate is binding the zinc atoms differently when compared to typical thiol complexes e.g. the VIM-2_**2b** complex. In both the VIM-2_**10b** and **10c** structures, the thioacetate interacts with Zn2 and the ND2 atom of Asn233 through the sulfur atom, with His263 and through a water molecule to the guanidinium group of Arg228 (Fig. 3B and C, respectively). In VIM-2_**10b** the S-atom is close to both zinc ions ($d(S_{ligand} \ldots Zn1/Zn2) = 2.96/3.22$ Å) (Fig. 3B), while for VIM-2_**10c**, the S to zinc distances are longer ($d(S_{ligand} \ldots Zn1/Zn2) = 3.29/4.02$ Å; Fig. 3C). In both structures, the phosphonic acid is adjacent to Trp87 and interacting with the side chain of Asn233. These findings differ from the reported CphA—mercaptophosphonic acid complex, in which the Zn was coordinated by two oxygen atoms of the phosphonic acid and not by the sulfur atom of the thiol [43]. However, CphA belongs to the B2 MBL subclass containing one zinc ion in the active site compared to two zinc ions for B1 MBLs, which may explain the observed differences. In addition, the benzene ring of compound **10b** is more parallel to Tyr67 compared to VIM-2_**2b** structures, and both Arg228 and the main chain of Gly232 are stacking at the opposite side, and His263 in a T-shaped orientation.

Furthermore, the position of residue Phe61 differs significantly between complexes of **2b** and **10b/c**. In the complexes of **10b** and **10c**, the residue Phe61 is moved and closed down on the inhibitors interacting with the phosphonic acid group, whereas in the **2b** structure Phe61 is in a slight more open conformation interacting with the ethyl groups (Fig. 4A).

2.5. Modeling of complexes with GIM-1 and NDM-1

The sequence identity between the three MBLs included in this study is 32% (VIM-2 versus NDM-1), 28% (VIM-2 versus GIM-1) or 24% (NDM-1 versus GIM-1) (Fig. S1). Low sequence identity is also found between the second shell sphere residues that constitute the active site together with the six conserved zinc binding residues (116, 118, 196, 120, 221, 263). The impact from these second shell interacting residues on ligand binding with GIM-1 and NDM-1 was examined by modeling the inhibitor binding based on the VIM-2 complexes obtained.

When superimposing the new VIM-2 complexes with inhibitors **2b**, **10c** and **10b** onto the GIM-1 structure (Fig. 4C, D) (PDB ID:

2YNW [50]), it becomes clear that the R2 binding sites accommodating the phenyl group of the inhibitors are very different. For GIM-1, both Trp228 and Tyr64 confine the R2 site making it smaller and more hydrophobic. Our reported IC_{50} values for compounds **2** and **10** are not significantly different for the longest (n = 4) compared to the shortest (n = 2) inhibitors in a series (Table 1). This indicates that similar favorable T-shaped stacking from Trp228 and cation-π interactions from Arg224 to the phenyl groups of the inhibitors are possible for all compounds within a series. Several conformations are described for Trp228 in the native GIM-1 crystal structures [50], which all can contribute to the described inhibitor interactions. Furthermore, residue 233 is a tyrosine in GIM-1 and the polar interactions observed in VIM-2_**2b**, **10b** and **10c** from Asn233 to the P=O group cannot be formed. Still the low IC_{50} of for **2a** of 0.18 μM and 64% inhibition towards GIM-1 (Table 1) tells that it is possible to inhibit GIM-1 in a cell based assay.

The new synthetized inhibitors are less efficient towards *E. coli* SNO3 cell with NDM-1, but **2a**, **2b** and **10a-c** show low IC_{50} values with pure enzyme (1.8–6.6 μM; Table 1). As with VIM-2 (and in contrast to GIM-1), NDM-1 has an Asn233 residue, which can bind the inhibitors through the P=O group as for VIM-2. However, hydrophobic stabilization of the phenyl rings of the inhibitors is limited for NDM-1 as the R2 binding site consists of Ala228 and Lys224, where the lysine residue is shorter than Arg228 (VIM-2) and Arg224 (GIM-1). Further, Phe63 in NDM-1 is too far away to reach down to the phenyl groups of the modeled **2b**, **10b** and **10c** inhibitor complexes (Fig. 4E). In the reported complex structure of NDM-1 with hydrolyzed ampicillin (PDB ID: 3Q6X; Fig. 4F), the substrate interacts with Ile64 and Val73 (in the R2 site), and the "R1" part of the ampicillin with Met60 and Gln119. The NDM-1 binding site is more hydrophobic and also different from both VIM-2 and GIM-1 with few conserved second shell residues, thus the design of an inhibitor hitting all three MBL targets is challenging.

3. Conclusion

Our bioisosteric approach on designing new metallo-β-lactamase inhibitors was found successful with low dose rate measurement for the **2** series of inhibitors (IC_{50} = 0.18–2.2 μM) towards all three enzymes, VIM-2, GIM-1 and NDM-1. For the cell-based assay with a β-lactamase-negative *E. coli* SNO3 cells inducing expression of one MBL, the best inhibitors were the **3** and **10** series. The three new crystal structures of VIM-2 with **2b**, **10b** or **10c,** reveal energetic favorable cation-π interactions from Arg228, and stacking from Tyr67 and Phe61 with the phenyl ring of the inhibitors. Asn233 in VIM-2 is also contributing with polar interactions to the P=O group (**2b**) and sulphur atom (**10b**, **10c**).
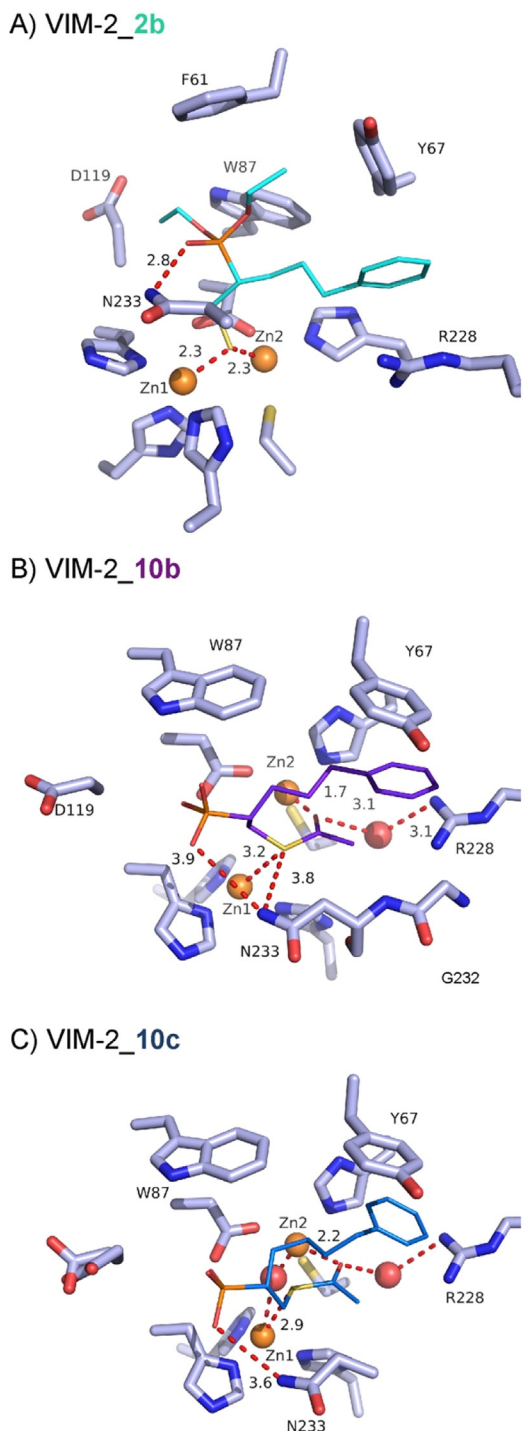
A) VIM-2_2b

B) VIM-2_10b

C) VIM-2_10c

Fig. 3. Interactions found in the VIM-2_**2b** (A), VIM-2_**10b** (B) and the VIM-2_**10c** (C) complexes. For the two latter (**10b** and **10c**), residue Phe61 is situated above the paper plane and left out of the figure for simplification.

Disappointingly, no synergistic effect was seen in *P. aeruginosa* nor in *K. pneumoniae* bacterial strains, but some effects on a clinical isolate from *E. coli* with VIM-29 were observed for **3b** and **10b** showing reduced MIC from 8–32 mg/L with only meropenem to 1 mg/L for meropenem in combination with inhibitor. A broad inhibitor hitting VIM-2, GIM-1 and NDM-1 was not found, but one promising hit is the thioacetate phosphonic acid **10b**, which seems to target both VIM-2 and NDM-1. The reported VIM-2_**10b**

structure is therefore a valuable starting point for a structure-guided design of an inhibitor targeting both VIM-2 and NDM-1 simultaneously.

4. Experimental

4.1. Chemistry

All reagents and solvents were purchased from commercial sources and used as supplied unless otherwise stated. Compounds **1c** and **17** were prepared according to the literature [36]. Reactions were monitored by thin-layer chromatography (TLC) with Merck pre-coated silica gel plates (60 F_{254}). Visualization was accomplished with either UV light or by immersion in potassium permanganate or phosphomolybdic acid (PMA) followed by light heating with a heating gun. Purification of reactions was carried out by flash column chromatography using silica gel from Merck (Silica gel 60, 0.040–0.063 mm). Analytical HPLC was carried out on a Purity analysis was carried out on Waters Acquity UPLC® BEH C18 (1.7 μm, 2.1 × 100 mm) column on a Waters Acquity I-class UPLC with Photodiode Array Detector. NMR spectra were obtained on a 400 MHz Bruker Avance III HD equipped with a 5 mm SmartProbe BB/1H (BB = 19F, 31P-15 N). Data are represented as follows: chemical shift, multiplicity (s = singlet, d = doublet, t = triplet, q = quartet, p = pentet, m = multiplet), coupling constant (J, Hz) and integration. Chemical shifts (δ) are reported in ppm relative to the residual solvent peak (CDCl$_3$: δ_H 7.26 and δ_C 77.16; Methanol-d$_4$: δ_H 3.31 and δ_C 49.00). ^{31}P NMR spectra were recorded using an insertion NMR tube filled with PPh$_3$ (δ = −5.4 ppm) solution in C$_6$D$_6$ as a reference. Positive ion electrospray ionization mass spectrometry was conducted on a Thermo electron LTQ Orbitrap XL spectrometer. IR spectra were recorded with Model Varian 7000e FT-IR spectrometer.

4.1.1. Preparation and spectroscopic data of 2-(Mercaptomethyl)-6-phenylhexanoic acid (1c)

The title compound **1c** was prepared as reported in the literature [36]. The final deacetylation was performed according to the general procedure (see chapter 4.1.5). The preceding thioacetate (1.67 mmol, 468 mg, 1 equiv) in methanol (6 mL) was treated with 1 M NaSMe in MeOH (3.4 mmol, 3.4 mL, 2 equiv). Reaction time was 1.5 h. Column chromatography (6% MeOH:CH$_2$Cl$_2$) gave the product **1c** as a white solid (1.23 mmol, 290 mg, 74%) of high purity (>95% as determined by HPLC). ^{1}H NMR (400 MHz, Chloroform-d) δ 10.85 (s, 1H), 7.30–7.16 (m, 4H), 2.79–2.74 (m, 1H), 2.68–2.60 (m, 2H), 1.75–1.66 (m, 4H), 1.53 (t, J = 8.5 Hz, 1H), 1.44 (q, J = 7.8 Hz, 2H). ^{13}C NMR (101 MHz, Chloroform-d) δ 180.7, 142.2, 128.4, 128.3, 125.8, 125.7, 49.0, 35.6, 31.2, 31.2, 30.9, 26.6, 25.6. HRMS (ESI): Calcd. for C$_{13}$H$_{17}$O$_2$S [M+H]$^+$ 237.0954; found 237.0944. The NMR and MS data were in accordance with the literature [36].

4.1.2. General procedure for the alkylation of triethyl phosphonoacetate (6a–c)

A solution of ethyl-2-(diethoxyphosphoryl) acetate **5** in DMF (25 mL/mol) was stirred at 0 °C. The base was added and the solution was continued to stir for 20 min before the alkyl halide was added drop wise. The reaction mixture was allowed to warm to room temperature and then heated at 60 °C for 18 h. After cooling the reaction mixture was acidified with 10% citric acid and extracted with diethyl ether (3 × 30 mL). The combined organic phases were washed with H$_2$O (3 × 30 mL), brine (1 × 30 mL) and dried over Na$_2$SO$_4$. The product **6a–c** was purified with column chromatography using 2:1 diethyl ether/pentane as eluent.
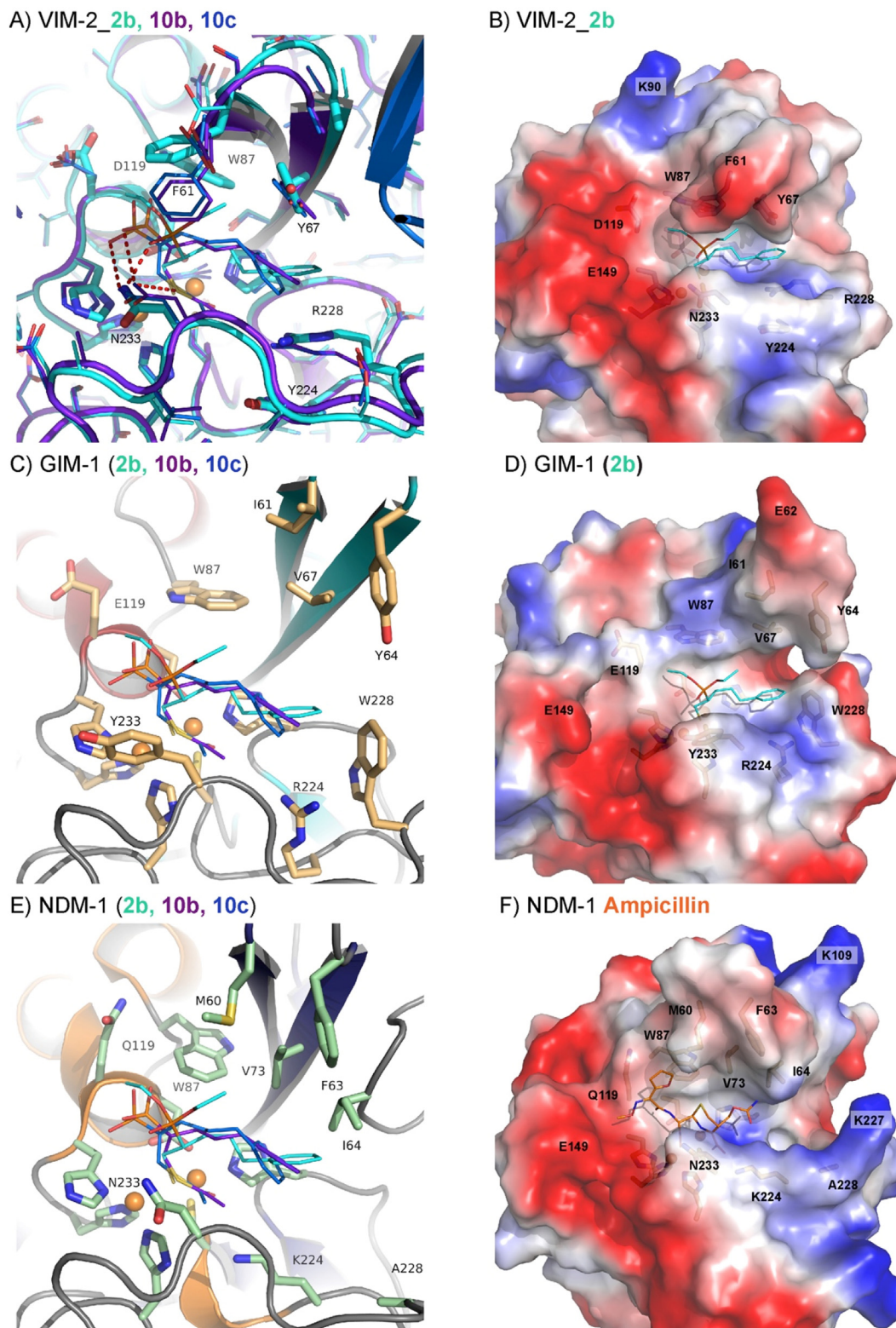
Fig. 4. Ribbon diagrams (left panels) and calculated electrostatic surfaces (right panels) of VIM-2 (A, B), GIM-1 (C, D) and NDM-1 (E, F). In panel F, the structure of ampicillin (orange) in complex with NDM-1 (PDB ID: 4RLO) is given. Residues discussed or being highly charged are labeled. (For interpretation of the references to colour in this figure legend, the reader is referred to the web version of this article.)

4.1.2.1. Ethyl 2-(diethoxyphosphoryl)-4-phenylbutanoate (6a). Potassium *tert*-butoxide (0.028 mol, 3.15 g, 1 equiv), ethyl 2-(diethoxyphosphoryl) acetate (0.028 mol, 6.30 g, 1 equiv) and 1-

bromo-2-phenylethane (0.028 mol, 5.18 g, 1 equiv) gave **6a** (0.018 mol, 5.76 g, 62%) as a pale yellow oil. ^{1}H NMR (400 MHz, Chloroform-*d*) δ 7.28—7.26 (m, 2H), 7.21—7.16 (m, 3H), 4.23—4.20

(m, 2H), 4.14–4.07 (m, 4H), 2.96 (ddd, J = 22.9, 11.0, 3.6 Hz, 1H), 2.79–2.69 (m, 1H), 2.64–2.56 (m, 1H), 2.35–2.26 (m), 2.18–2.12 (m, 1H), 1.30–1.28 (m, 9H). ^{13}C NMR (101 MHz, Chloroform-d) δ 169.5 (d, J = 5.0 Hz), 140.9, 128.9 (d, J = 10.7 Hz), 126.7, 63.2 (dd, J = 8.4, 6.7 Hz), 61.9, 46.2, 44.9, 34.9 (d, J = 15.4 Hz), 29.1 (d, J = 4.4 Hz), 16.9 (dd, J = 6.1, 2.3 Hz), 14.7. ^{31}P NMR (162 MHz, Chloroform-d): δ 23.0. HRMS (ESI): Calcd. for $C_{16}H_{26}O_5P$ [M+H]$^+$ 329.1512; found 329.1519.

4.1.2.2. Ethyl 2-(diethoxyphosphoryl)-5-phenylpentanoate (6b). Potassium *tert*-butoxide (0.064 mol, 7.18 g, 0.8 equiv), ethyl 2-(diethoxyphosphoryl) acetate (0.08 mol, 20.01 g, 1 equiv) and 1-bromo-3-phenylpropane (0.064 mol, 12.71 g, 0.8 equiv) gave **6b** (0.046 mol, 15.89 g, 73%) as a pale yellow oil. ^{1}H NMR (400 MHz, Chloroform-d) δ 7.29–7.24 (m, 2H), 7.19–7.14 (m, 3H), 4.28–4.08 (m, 6H), 2.96 (ddd, J = 22.7, 10.9, 3.8 Hz, 1H), 2.63 (t, J = 7.8 Hz, 2H), 2.07–2.02 (m, 1H), 1.92–1.89 (m, 1H), 1.72–1.65 (m, 2H), 1.34–1.26 (m, 9H). ^{13}C NMR (101 MHz, Chloroform-d) δ 169.1 (d, J = 4.8 Hz), 141.8 (d, J = 29.8 Hz), 128.3–128.2 (m), 125.8 (d, J = 29.8 Hz), 62.6 (dd, J = 9.1, 6.6 Hz), 61.3, 46.3, 44.9, 35.3, 30.1 (d, J = 14.9 Hz), 26.6 (d, J = 4.8 Hz), 16.3 (dd, J = 5.9, 2.7 Hz), 14.1. ^{31}P NMR (162 MHz, Chloroform-d): δ 23.1. HRMS (ESI): Calcd. for $C_{17}H_{27}O_5NaP$ [M+Na]$^+$ 365.1488; found 365.1484.

4.1.2.3. Ethyl 2-(diethoxyphosphoryl)-6-phenylhexanoate (6c). Potassium *tert*-butoxide (0.014 mol, 1.55 g, 0.7 equiv), ethyl-2-(diethoxyphosphoryl) acetate (0.019 mol, 4.25 g, 1 equiv) and 1-bromo-4-phenylbutane (0.013 mmol, 2.83 g, 0.7 equiv) gave **6c** (0.009 mol, 3.37 g, 73%) as a yellow oil. ^{1}H NMR (400 MHz, Chloroform-d) δ 7.33–7.28 (m, 2H), 7.22–7.15 (m, 3H), 4.27–4.12 (m, 6H), 2.96 (ddd, J = 22.5, 11.0, 3.8 Hz, 1H), 2.65–2.58 (m, 2H), 1.72–1.68 (m, 1H), 1.68–1.65 (m, 1H), 1.38–1.36 (m, 2H) 1.3–1.25 (m, 11H). ^{13}C NMR (101 MHz, Chloroform-d) δ 169.3 (d, J = 4.8 Hz), 142.2, 128.3 (d, J = 8.7 Hz), 125.7, 62.7 (t, J = 6.6, 14.6 Hz), 61.3, 46.5, 45.2, 35.5, 30.9, 28.1 (d, J = 15.0 Hz), 26.9 (d, J = 4.9 Hz), 16.4 (dd, J = 6.1, 3.2 Hz), 14.2. ^{31}P NMR (162 MHz, Chloroform-d): δ 23.3. HRMS (ESI): Calcd. for $C_{18}H_{30}O_5P$ [M+H]$^+$ 357.1825; found 357.1822.

4.1.3. General procedure for the reduction of alkylated triethyl phosphonoacetate (7a–c)

LiBH$_4$ was dissolved in THF (2 mL/mmol) at 0 °C and slowly added to the ester **6a–c** in THF at 0 °C. The suspension was stirred at room temperature for 30 min and irradiated at 80 °C for 10 min. The mixture was cooled to RT and slowly diluted with MeOH and stirred for 30 min until excess of the LiBH$_4$ was quenched. The mixture was acidified with 10% citric acid, saturated with NaCl and the product was extracted with diethyl ether. The organics were dried over Na$_2$SO$_4$, filtered and concentrated in vacuum. The product **3a–c** was purified with column chromatography with 5% MeOH:CH$_2$Cl$_2$.

4.1.3.1. Diethyl 1-hydroxy-4-phenylbutan-2-ylphosphonate (7a). Ethyl 2-(diethoxyphosphoryl)-4-phenylbutanoate **6a** (1.6 mmol, 0.53 g, 1 equiv) and LiBH$_4$ (4.8 mmol, 0.12 g, 3 equiv) gave **7a** (1.0 mmol, 0.28 g, 60%) as a colorless oil. ^{1}H NMR (400 MHz, Chloroform-d) δ 7.31–7.26 (m, 2H), 7.21–7.18 (m, 3H), 4.14–4.07 (m, 4H), 3.89–3.79 (m, 2H), 3.15–3.12 (m, 1H), 2.81 (ddd, J = 14.5, 9.2, 5.7 Hz, 1H), 2.69 (ddd, J = 13.8, 9.4, 6.6 Hz, 1H), 2.01–1.98 (m, 2H), 1.97–1.83 (m, 1H), 1.35–1.29 (m, 6H). ^{13}C NMR (101 MHz, Chloroform-d) δ 141.1, 128.4 (d, J = 5.7 Hz), 126.1, 61.9 (t, J = 6.7 Hz), 60.7 (d, J = 5.5 Hz), 39.1, 37.7, 33.5 (d, J = 11.1 Hz), 27.0 (d, J = 3.5 Hz), 16.5 (t, J = 5.5 Hz). ^{31}P NMR (162 MHz, Chloroform-d): δ 33.3. HRMS (ESI) Calcd. for $C_{14}H_{24}O_4P$ [M+H]$^+$ 287.1407; found 287.1408.

4.1.3.2. Diethyl 1-hydroxy-5-phenylpentane-2-ylphosphonate (7b). Ethyl 2-(diethoxyphosphoryl)-5-phenylpentanoate **6b** (4.7 mmol, 1.60 g, 1 equiv) and LiBH$_4$ (0.012 mol, 255 mg, 2.5 equiv) gave **7b** (4.5 mmol, 1.34 g, 95%) as a colorless oil. ^{1}H NMR (400 MHz, Chloroform-d) δ 7.29–7.25 (m, 2H), 7.19–7.16 (m, 3H), 4.15–4.08 (m, 4H), 3.82–3.77 (m, 2H), 3.46 (s, 1H), 2.62 (t, J = 7.4 Hz, 2H), 1.81–1.71 (m, 1H), 1.68–1.66 (m, 2H), 1.66–1.50 (m, 1H), 1.31 (m, 6H). ^{13}C NMR (101 MHz, Chloroform-d) δ 141.8, 128.3 (d, J = 5.7 Hz), 125.7, 61.8 (dd, J = 13.1, 6.8 Hz), 60.5 (d, J = 4.4 Hz), 39.9, 38.5, 35.6, 29.2 (d, J = 10.4 Hz), 25.1 (d, J = 3.7 Hz), 16.4 (d, J = 5.5 Hz). ^{31}P NMR (162 MHz, Chloroform-d): δ 33.0. HRMS (ESI) Calcd. for $C_{15}H_{26}O_4P$ [M+H]$^+$ 301.1563; found 301.1566.

4.1.3.3. Diethyl 1-hydroxy-6-phenylhexane-2-ylphosphonate (7c). Ethyl 2-(diethoxyphosphoryl)-6-phenylhexanoate **6c** (4.21 mmol, 1.5 g, 1 equiv) and LiBH$_4$ (10.53 mmol, 229 mg, 2.5 equiv) gave **7c** (2.34 mmol, 737 mg, 56%) as a colorless oil. ^{1}H NMR (400 MHz, Chloroform-d) δ 7.21–7.17 (m, 2H), 7.11–7.08 (m, 3H), 4.08–4.02 (m, 4H), 3.78–3.65 (m, 2H), 2.56–2.52 (m, 2H), 1.91–1.87 (m, 1H), 1.63–1.53 (m, 3H), 1.46–1.44 (m, 2H), 1.35–1.34 (m, 1H), 1.25 (t, J = 7.1 Hz, 6H). ^{13}C NMR (101 MHz, Chloroform-d) δ 142.4, 128.5–128.4 (m), 125.9, 62.1 (dd, J = 13.6, 6.9 Hz), 60.9 (d, J = 5.7 Hz), 40.0, 38.7, 35.8, 31.4, 27.3 (d, J = 11.0 Hz), 25.3 (d, J = 3.8 Hz), 16.6. ^{31}P NMR (162 MHz, Chloroform-d): δ 33.3. HRMS (ESI): Calcd. for $C_{16}H_{28}O_4P$ [M+H]$^+$ 315.1720; found 315.1723.

4.1.4. General procedure for thioacetylation (8a–c)

Compound **7a–c** (1 equiv) was dissolved in CH$_2$Cl$_2$ (5 mL/mmol) and added triethylamine (1.05 equiv) and a catalytic amount of 4-dimethylaminopyridine (DMAP). The mixture was stirred for 5 min at RT, before methanesulfonyl chloride (1.05 equiv) was slowly added. The reaction mixture was stirred for 3–24 h at RT. The solvent was evaporated, and the remaining crude was quenched with 100 mL aq. NH$_4$Cl and extracted with diethyl ether, dried over Na$_2$SO$_4$, filtered, and evaporated. To the crude was added an excess (7–10 equiv) of 2 M potassium thioacetate in DMF and stirred overnight at RT. The brown suspension was quenched with aq. NH$_4$Cl (100 mL) and the product was extracted with diethyl ether (3 × 30 mL). The combined organic layers were washed with H$_2$O (3 × 50 mL), dried over Na$_2$SO$_4$ and concentrate to yield an orange oil. The crude was purified with column chromatography using 5–15% MeOH:CH$_2$Cl$_2$ as eluent.

4.1.4.1. S-2-(diethoxyphosphoryl)-4-phenylbutyl ethanethioate (8a). Diethyl 1-hydroxy-4-phenylbutan-2-ylphosphonate **7a** (2.8 mmol, 825 mg, 1 equiv), triethylamine (2.9 mmol, 355 mg, 1.05 equiv), methanesulfonyl chloride (2.9 mmol, 355 mg, 1.05 equiv), DMAP (catalytic amount) and potassium thioacetate (20.3 mmol, 2.31 g, 7 equiv) gave **8a** (1.5 mmol, 520 mg, 54%) as an orange oil. ^{1}H NMR (400 MHz, Chloroform-d) δ 7.33–7.30 (m, 2H), 7.25–7.22 (m, 3H), 4.23–4.13 (m, 4H), 3.44–3.39 (m, 1H), 3.08–3.05 (m, 1H), 2.85–2.81 (m, 2H), 2.37 (s, 3H), 2.10–2.05 (m, 2H), 1.93–1.91 (m, 1H), 1.41–1.36 (m, 6H). ^{13}C NMR (101 MHz, Chloroform-d) δ 195.3, 141.4, 128.5 (d, J = 12.7 Hz), 126.0, 61.9 (dd, J = 6.8, 2.5 Hz), 36.4, 35.1, 33.5 (d, J = 7.5 Hz), 30.6, 29.6 (d, J = 3.3 Hz), 28.3 (d, J = 2.0 Hz), 16.5 (d, J = 5.9 Hz). ^{31}P NMR (162 MHz, Chloroform-d): δ 30.3. HRMS (ESI): Calcd. for $C_{16}H_{26}O_4PS$ [M+H]$^+$ 345.1285; found 345.1289.

4.1.4.2. S-2-(diethoxyphosphoryl)-5-phenylpentyl ethanethioate (8b). Diethyl 1-hydroxy-5-phenylpentane-2-ylphosphonate **7b** (0.93 mmol, 289 mg, 1 equiv), triethylamine (0.98 mmol, 111 mg, 1.05 equiv), methanesulfonyl chloride (0.98 mmol, 111 mg, 1.05 equiv), DMAP (catalytic amount) and potassium thioacetate (9.3 mmol, 1.06 g, 10 equiv) gave **8b** (0.32 mmol, 114 mg, 34%) as an

orange oil. ^{1}H NMR (400 MHz, Chloroform-*d*) δ 7.22–7.18 (m, 2H), 7.12–7.08 (m, 3H), 4.07–4.00 (m, 4H), 3.26 (ddd, *J* = 15.2, 13.9, 5.1 Hz, 1H), 2.92 (ddd, *J* = 13.9, 12.0, 8.2 Hz, 1H), 2.54 (t, *J* = 7.3 Hz, 2H), 2.25 (s, 3H), 1.99–1.86 (m, 1H), 1.76–1.70 (m, 3H), 1.63–1.43 (m, 1H), 1.27–1.23 (m, 6H). ^{13}C NMR (101 MHz, Chloroform-*d*) δ 195.1, 141.8, 128.3 (dd, *J* = 16.7, 1.9 Hz), 125.7, 61.8 (t, *J* = 6.9 Hz), 37.0, 35.7–35.4 (m), 30.4 (d, *J* = 2.5 Hz), 28.9 (dd, *J* = 7.3, 2.3 Hz), 28.3 (d, *J* = 1.9 Hz), 27.4 (d, *J* = 3.7 Hz), 16.4 (d, *J* = 5.8 Hz). ^{31}P NMR (162 MHz, Chloroform-*d*): δ 30.5. HRMS (ESI): Calcd. for $C_{17}H_{28}O_4PS$ [M+H]$^+$ 359.1440; found 359.1449.

*4.1.4.3. S-2-(diethoxyphosphoryl)-6-phenylhexyl ethanethioate (**8c**).* Diethyl 1-hydroxy-6-phenylhexane-2-ylphosphonate **7c** (13 mmol, 4.20 g, 1 equiv), triethylamine (0.014 mmol, 1.42 g, 1.05 equiv), methanesulfonyl chloride (1.34 mmol, 152 mg, 1.05 equiv)), DMAP (catalytic amount) and potassium thioacetate (0.14 mmol, 15.98 g, 10 equiv) gave **8c** (9.4 mmol, 3.502 g, 71%) as an orange oil. ^{1}H NMR (400 MHz, Chloroform-*d*) δ 7.34–7.30 (m, 2H), 7.24–7.21 (m, 3H), 4.18–4.15 (m, 4H), 3.38 (ddd, *J* = 15.2, 13.8, 5.0 Hz, 1H), 3.03 (ddd, *J* = 13.9, 11.9, 8.2 Hz, 1H), 2.67 (t, *J* = 7.6 Hz, 2H), 2.38 (s, 3H), 2.06–1.97 (m, 1H), 1.83–1.77 (m, 1H), 1.69–1.62 (m, 3H), 1.62–1.56 (m, 2H), 1.40–1.36 (m, 6H). ^{13}C NMR (101 MHz, Chloroform-*d*) δ 195.4, 142.5, 128.4 (d, *J* = 13.2 Hz), 125.7, 61.9 (dd, *J* = 6.9, 5.0 Hz), 37.2, 35.7 (d, *J* = 8.9 Hz), 31.5, 30.6, 28.5 (d, *J* = 1.8 Hz), 27.9 (d, *J* = 3.5 Hz), 27.1 (d, *J* = 7.4 Hz), 16.5 (d, *J* = 6.0 Hz). ^{31}P NMR (162 MHz, Chloroform-*d*): δ 31.1. HRMS (ESI): calcd. For $C_{18}H_{26}O_4PS$ [M+H]$^+$ 373.1602; found 373.1289.

*4.1.5. Deacetylation of thioacetates (preparation of **1c**, **2a**–**c** and **4**)*
    Except for **2a**, the following general procedure was applied. To a stirred solution of *thioacetate* (**8** or **15**) (1 equiv) in methanol (6 mL) at −20 °C was added sodiumthiomethoxide, NaSMe (1 M solution in MeOH, 1 equiv). The reaction mixture was stirred for 30 min at −20 °C, before aqu. HCl (0.1 M) was added. The reaction mixture was extracted with DCM (3 × 30 mL), the combined organic layers were washed with brine, dried over $MgSO_4$, filtered and concentrate. The resulting crude was purified by column chromatography.

*4.1.5.1. Diethyl 1-mercapto-4-phenylbutan-2-ylphosphonate (**2a**).* According to the reported procedure [38], a 0.1 M NaOMe/MeOH solution (3 mmol, 3 mL, 2 equiv) was added to thioacetate **8a** (1.5 mmol, 0.52 g, 1 equiv) at 0 °C. The resulting mixture was stirred for 15 min at rt under H$_2$ and concentrated. Aq. NH$_4$Cl (30 mL) and 0.1 M HCl (10 mL) were added to the crude and the product was extracted with diethyl ether. The combined organics were dried and concentrated. Repeated column chromatography (5–20% MeOH: CH$_2$Cl$_2$ and 3:1 EtOAc:Et$_2$O) gave **2a** (0.46 mmol, 139 mg, 30%) as a slightly orange oil. ^{1}H NMR (400 MHz, Methanol-*d$_4$*) δ 7.33–7.29 (m, 2H), 7.26–7.20 (m, 3H), 4.18–4.10 (m, 4H), 3.04–2.92 (m, 1H), 2.86–2.72 (m, 4H), 2.15–2.01 (m, 3H), 1.71 (t, *J* = 8.3 Hz, 1H), 1.37–1.33 (m, 6H). ^{13}C NMR (101 MHz, Methanol-*d$_4$*) δ 142.9, 129.7, 127.3, 63.7 (dd, *J* = 7.1, 1.9 Hz), 40.5, 39.1, 34.4 (d, *J* = 8.2 Hz), 30.2 (d, *J* = 3.2 Hz), 23.9 (d, *J* = 2.6 Hz), 16.9 (d, *J* = 5.8 Hz). ^{31}P NMR (162 MHz, Choroform-*d*) δ 32.9. HRMS (ESI): Calcd. for $C_{16}H_{28}O_3PS$ [M+H]$^+$ 331.1491; found 331.1494.

*4.1.5.2. Diethyl 1-mercapto-5-phenylpentan-2-ylphosphonate (**2b**).* Thioacetate **8b** (0.56 mmol, 0.20 g, 1 equiv) in methanol and 1 M NaSMe in MeOH (0.6 mmol, 0.6 mL, 1 equiv) gave **2b** (0.41 mmol, 130 mg, 74%) as white oil after purification with column chromatography (5–20% MeOH: CH$_2$Cl$_2$). ^{1}H NMR (400 MHz, Chloroform-*d*) δ 7.29–7.25 (m, 2H), 7.19–7.15 (m, 3H), 4.12–4.04 (m, 4H), 2.96–2.85 (m, 1H), 2.69–2.62 (m, 3H), 1.98–1.93 (m, 1H), 1.80–1.76 (m, 4H), 1.65 (t, *J* = 8.4 Hz, 1H), 1.32–1.28 (m, 6H). ^{13}C NMR (101 MHz, Chloroform-*d*) δ 142.0, 128.5 (d, *J* = 8.8 Hz), 125.9, 61.9

(dd, *J* = 7.3, 3.1 Hz), 40.4, 38.9, 35.9, 28.9 (d, *J* = 8.2 Hz), 26.7 (d, *J* = 3.6 Hz), 23.7 (d, *J* = 2.7 Hz), 16.6 (d, *J* = 6.2 Hz). ^{31}P NMR (162 MHz, Chloroform-*d*) δ 31.9. HRMS (ESI): Calcd. for $C_{15}H_{26}O_3PS$ [M+H]$^+$ 317.1335; found 317.1337.

*4.1.5.3. Diethyl 1-mercapto-6-phenylhexan-2-ylphosphonate (**2c**).* Thioacetate **8c** (1.07 mmol, 400 mg, 1 equiv) in methanol and 1 M NaSMe in MeOH (1.1 mmol, 1.1 mL, 1 equiv) gave **2c** (0.82 mmol, 270 mg, 77%) as a colorless oil after purification with column chromatography (5–20% MeOH: CH$_2$Cl$_2$). ^{1}H NMR (400 MHz, Chloroform-*d*) δ 7.28–7.23 (m, 2H), 7.17–7.15 (d, *J* = 6.8 Hz, 3H), 4.12–4.05 (m, 4H), 2.94–2.83 (m, 1H), 2.70–2.60 (m, 3H), 1.98–1.80 (m, 1H), 1.76–1.66 (m, 5H), 1.60–1.43 (m, 2H), 1.30 (t, *J* = 7.0 Hz, 6H). ^{13}C NMR (101 MHz, Chloroform-*d*) δ 142.5, 128.5 (d, *J* = 11.5 Hz), 125.8, 61.8 (d, *J* = 6.9 Hz), 40.3, 38.9, 35.7 (d, *J* = 1.9 Hz), 31.4, 26.9–26.8 (m), 23.6 (d, *J* = 2.3 Hz), 16.6 (d, *J* = 5.9 Hz). ^{31}P NMR (162 MHz, Chloroform-*d*) δ 31.5. HRMS (ESI): Calcd. for $C_{16}H_{28}O_3PS$ [M+H]$^+$ 331.1486; found 331.1491.

*4.1.5.4. 5-Phenyl-2-(1H-tetrazol-5-yl)pentane-1-thiol (**4**).* Thioacetate **15b** (0.1 mmol, 30 mg, 1 equiv) in methanol was treated with 1 M NaSMe in MeOH (0.2 mmol, 0.2 mL, 2 equiv). The reaction time was 1.5 h at RT. Column chromatography (3% MeOH: CH$_2$Cl$_2$) provided 4 as white solid (0.073 mmol, 18.1 mg, 73%) with high purity (>95% as determined by HPLC). ^{1}H NMR (400 MHz, Methanol-*d$_4$*) δ 7.19–7.04 (m, 5H), 3.45–3.43 (m, 1H), 3.04–2.95 (m, 2H), 2.56 (q, *J* = 7.6 Hz, 2H), 1.82 (ddd, *J* = 35.0, 8.0, 4.1 Hz, 2H), 1.75–1.72 (m, 2H), 1.49–1.36 (m, 2H). ^{13}C NMR (101 MHz, Methanol-*d$_4$*) δ 158.3, 141.5, 127.9, 125.5, 41.1, 35.3, 34.8, 32.7, 28.5. HRMS (ESI): Calcd. for $C_{12}H_{17}N_4S$ [M+H]$^+$ 249.1170; found 249.1168.

*4.1.6. General procedure for the hydrolysis of phosphonic esters (preparation of **3**, **9** and **10**)*
    Bromotrimethylsilane (3 equiv) was added drop wise to **2**, **7** or **8** (1 equiv) in 10 mL dry CH$_2$Cl$_2$ under argon. The mixture was stirred overnight at room temperature. The solvent and excess TMSBr were removed under reduced pressure, MeOH (0.2 mL/mmol of substrate) was added and the reaction mixture was stirred for 1 h at RT. The reaction mixture was evaporated to dryness. The crude **3**, **9** or **10** was obtained as viscous oil. Crude product was dissolved in minimal volume of EtOAc and cold pentane was added resulting in the separation of compound as oily or crystalline material. The pentane layer was discarded and the remaining compound was dried under vacuum.

*4.1.6.1. 1-Hydroxy-4-phenylbutan-2-ylphosphonic acid (**9a**).* Diethyl 1-hydroxy-4-phenylbutyl-2-ylphosphonate **7a** (0.31 mmol, 95 mg, 1 equiv) and TMSBr (140 mg) gave crude **9a** (77 mg) as a colorless oil. A small batch (30 mg) was dissolved in 2–3 drops of EtOAc and washed with cold pentane, afforded the pure product **9a** (0.086 mmol, 20 mg, 76%). ^{1}H NMR (400 MHz, Chloroform-*d*) δ 8.65 (s, 2H), 7.15–7.08 (m, 5H), 3.84–3.80 (m, 2H), 2.69–2.58 (m, 2H), 2.02–1.80 (m, 2H), 1.78–1.73 (m, 1H). ^{13}C NMR (101 MHz, Methanol-*d$_4$*) δ 142.0, 128.0 (d, *J* = 13.0 Hz), 125.5, 60.3, 40.5, 39.2, 33.6 (d, *J* = 8.3 Hz), 28.1 (d, *J* = 3.2 Hz), 22.8. ^{31}P NMR (162 MHz, Methanol-*d$_4$*) δ 26.1. HRMS (ESI): Calcd. for $C_{10}H_{16}O_4P$ [M+H]$^+$ 231.0781; found: 231.0779.

*4.1.6.2. 1-Hydroxy-5-phenylpentan-2-ylphosphonic acid (**9b**).* Diethyl 1-hydroxy-5-phenylpentan-2-ylphosphonate **7b** (0.36 mmol, 0.1 g, 1 equiv) and TMSBr (1.06 mmol, 0.16 g, 3 equiv) gave crude **9b** (110 mg) as a colourless oil. A small batch (64 mg) was dissolved in 2–3 drops of EtOAc and washed with cold pentane, afforded the pure product **9b** (0.16 mmol, 39 mg, 61%). ^{1}H NMR (400 MHz, Methanol-*d$_4$*) δ 7.29–7.15 (m, 5H), 3.92 (ddd, *J* = 14.3, 11.0, 4.9 Hz,

1H), 3.73–3.64 (m, 1H), 2.68–2.63 (m, 2H), 1.98–1.69 (m, 5H). ^{13}C NMR (101 MHz, Methanol-d_4) δ 142.2, 127.9 (d, J = 15.9 Hz), 125.3, 60.4, 40.9, 39.5, 35.7, 29.6 (d, J = 8.3 Hz), 25.8 (d, J = 3.4 Hz). ^{31}P NMR (162 MHz, Methanol-d_4) δ 31.1. HRMS (ESI): Calcd. for $C_{11}H_{18}O_4P$ [M+H]$^+$ 245.0937; found 245.0936.

4.1.6.3. 1-Hydroxy-5-phenylpentane-2-ylphosphonic acid (9c). Diethyl 1-hydroxy-5-phenylpentan-2-ylphosphonate **7c** (0.36 mmol, 100 mg, 1 equiv) and TMSBr (0.95 mmol, 150 mg, 3 equiv) gave crude **9c** (110 mg) as colorless oil. A small batch (38 mg) was dissolved in 2–3 drops of EtOAc and washed with cold pentane, afforded the pure product **9c** (21 mg, 0.081 mmol, 55%). ^{1}H NMR (400 MHz, Chloroform-d) δ 8.22 (s, 2H), 7.27–7.20 (m, 2H), 7.15–7.10 (m, 3H), 3.91–3.74 (m, 2H), 2.57–2.53 (m, 2H), 1.94–1.73 (m, 1H), 1.69–1.56 (m, 1H), 1.55–1.38 (m, 5H). ^{13}C NMR (101 MHz, Methanol-d_4) δ 142.4, 127.9 (d, J = 13.5 Hz), 125.2, 60.3, 40.9, 39.5, 35.3, 31.5, 27.2 (d, J = 8.5 Hz), 25.7 (d, J = 3.4 Hz). ^{31}P NMR (162 MHz, Methanol-d_4) δ 32.0. HRMS (ESI): Calcd. for $C_{12}H_{19}O_4PNa$ [M+H]$^+$ 281.0916; found 281.0913.

4.1.6.4. 1-Acetylthio-4-phenylbutan-2-ylphosphonic acid, (10a). S-2-(diethoxyphosphoryl)-4-phenylbutyl ethanethioate **8a** (0.77 mmol, 268 mg, 1 equiv) and TMSBr (2.31 mmol, 353 mg, 3 equiv) gave crude **10a** (232 mg) as an orange oil. The crude was dissolved in 2–3 drops of EtOAc and washed with cold pentane, afforded the pure product **10a** (0.69 mmol, 201 mg, 91%). ^{1}H NMR (400 MHz, Methanol-d_4) δ 7.26–7.22 (m, 2H), 7.19–7.14 (m, 3H), 3.44–3.36 (m, 1H), 3.04 (ddd, J = 13.8, 10.4, 8.4 Hz, 1H), 2.79–2.76 (m, 2H), 2.30 (s, 3H), 2.07–1.81 (m, 3H). ^{13}C NMR (101 MHz, Methanol-d_4) δ 195.5, 141.8 (d, J = 17.5 Hz), 128.1–128.0 (m), 125.5, 40.4, 39.0, 37.2, 35.8, 33.1 (t, J = 8.0 Hz), 29.7 (d, J = 2.9 Hz), 28.9 (dd, J = 10.7, 2.5 Hz), 28.0, 22.9. ^{31}P NMR (162 MHz, Methanol-d_4) δ 30.4. HRMS (ESI): Calcd. for $C_{12}H_{18}O_4PS$ [M+H]$^+$ 289.0658; found 289.0660.

4.1.6.5. 1-(Acetylthio)-5-phenylpentan-2-ylphosphonic acid, (10b). S-2-(diethoxyphosphoryl)-5-phenylpentan ethanethioate **8b** (0.53 mmol, 190 mg, 1 equiv) and TMSBr (1.58 mmol, 242 mg, 3 equiv) gave crude **10b** (207 g) as an orange oil. The crude was dissolved in 2–3 drops of EtOAc and washed with cold pentane, afforded the pure product **10b** (0.37 mmol, 113 mg, 71%). ^{1}H NMR (400 MHz, Methanol-d_4) δ 7.25–7.13 (m, 5H), 3.39–3.30 (m, 1H), 3.00 (ddd, J = 14.0, 10.9, 8.5 Hz, 1H), 2.58 (t, J = 7.3 Hz, 2H), 2.27 (s, 3H), 1.94–1.56 (m, 6H). ^{13}C NMR (101 MHz, Methanol-d_4) δ 195.4, 141.9, 128.0 (d, J = 18.7 Hz), 125.4, 37.8, 36.4, 35.4, 29.0 (d, J = 7.4 Hz), 28.0, 27.5 (d, J = 3.1 Hz). ^{31}P NMR (162 MHz, Methanol-d_4) δ 30.8. HRMS (ESI): Calcd. for $C_{13}H_{20}O_4PS$ [M+H]$^+$ 303.0814; found 303.0818.

4.1.6.6. 1-(Acetylthio)-6-phenylhexan-2-ylphosphonic acid, (10c). S-2-(diethoxyphosphoryl)-6-phenylhexyl ethanethioate, **8c** (0.478 mmol, 0.178 g, 1 equiv) and TMSBr (1.434 mmol, 0.219 g, 3 equiv) gave crude **10c** (113 mg) as an orange oil. The crude was dissolved in 2–3 drops of EtOAc and washed with cold pentane, afforded the pure product **10c** (0.31 mmol, 98 mg, 65%). ^{1}H NMR (400 MHz, Methanol-d_4) δ 7.26–7.20 (m, 3H), 7.19–7.12 (m, 2H), 3.39–3.33 (m, 1H), 3.04 (ddd, J = 13.8, 10.8, 8.6 Hz, 1H), 2.65–2.58 (m, 3H), 2.30 (s, 3H), 1.96–1.89 (m, 1H), 1.82–1.72 (m, 4H), 1.64–1.59 (m, 1H). ^{13}C NMR (101 MHz, Methanol-d_4) δ 195.5, 141.9, 128.1–127.8 (m), 125.3, 40.9, 39.6, 37.8, 36.4, 35.5 (d, J = 11.7 Hz), 29.2–28.8 (m), 28.1, 27.5 (d, J = 3.1 Hz), 26.7 (d, J = 3.0 Hz), 23.0. ^{31}P NMR (162 MHz, Methanol-$d4$) δ 31.5. HRMS (ESI): Calcd. for $C_{14}H_{20}O_4PS$ [M+H]$^+$ 315.0820; found 315.0817.

4.1.6.7. 1-Sulfanyl-4-phenylbutan-2-ylphosphonic acid (3a). Diethyl 1-sulfanyl-4-phenylbutan-2-ylphosphonate **2a** (0.14 mmol, 43 mg, 1 equiv) and TMSBr (0.43 mmol, 65 mg, 3 equiv) gave crude **3a** (38 mg) as an orange oil. The crude was dissolved in 2–3 drops of EtOAc and washed with cold pentane, afforded the pure product **3a** (0.13 mmol, 33 mg, 96%). ^{1}H NMR (400 MHz, Chloroform-d) δ 9.05 (s, 2H), 7.28–7.19 (m, 5H), 3.05–2.94 (m, 1H), 2.78–2.74 (m, 3H), 2.14–2.07 (m, 3H), 1.56 (t, J = 8.4 Hz, 1H). ^{13}C NMR (101 MHz, Methanol-d_4) δ 141.8, 128.1 (d, J = 12.3 Hz), 125.6, 40.4, 39.0, 33.1 (d, J = 7.5 Hz), 28.9, 22.9. ^{31}P NMR (162 MHz, Methanol-d_4) δ 30.43. HRMS (ESI): Calcd. for $C_{10}H_{16}O_3PS$ [M+H]$^+$ 247.0552; found 247.0552.

4.1.6.8. 1-Sulfanyl-5-phenylpentan-2-ylphosphonic acid (3b). Diethyl 1-sulfanyl-5-phenylpentan-2-ylphosphonate **2b** (0.05 mmol, 15 mg, 1 equiv) and TMSBr (0.14 mmol, 22 mg, 3 equiv) gave crude **3b** as an orange oil. The crude was dissolved in 2–3 drops of EtOAc and washed with cold pentane, afforded the pure product **3b** (0.04 mmol, 11 mg, 90%). ^{1}H NMR (400 MHz, Methanol-d_4) δ 7.27–7.18 (m, 4H), 7.16–7.12 (m, 1H), 2.97 (ddd, J = 17.8, 13.7, 3.8 Hz, 1H), 2.66–2.60 (m, 3H), 1.91–1.78 (m, 5H). ^{13}C NMR (101 MHz, Methanol-d_4) δ 142.9, 128.8 (d, J = 16.9 Hz), 126.1 (d, J = 3.3 Hz), 41.8, 40.4, 36.3, 29.9(d, J = 7.4 Hz), 27.5 (d, J = 2.5 Hz), 23.8. ^{31}P NMR (162 MHz, Methanol-d_4) δ 30.12. HRMS (ESI): Calcd. for $C_{11}H_{18}O_3PS$ [M+H]$^+$ 261.0709; found 261.0712.

4.1.6.9. 1-Sulfanyl-6-phenylhexan-2-ylphosphonic acid, (3c). Diethyl 1-sufanyl-6-phenylhexan-2-ylphosphonate **2c** (0.30 mmol, 100 mg, 1 equiv) and TMSBr (0.91 mmol, 144 mg, 3 equiv) gave crude **3c** as an orange oil. The crude was dissolved in 2–3 drops of EtOAc and washed with cold pentane, afforded the pure product **3c** (0.29 mmol, 81 mg, 98%). ^{1}H NMR (400 MHz, Chloroform-d) δ 8.59 (s, 2H), 7.29–7.25 (m, 2H), 7.19–7.16 (m, 3H), 2.98 (ddd, J = 20.0, 13.9, 4.6 Hz, 1H), 2.75–2.63 (m, 1H), 2.62 (dd, J = 8.8, 6.4 Hz, 2H), 2.11–2.02 (m, 1H), 1.83 (ddd, J = 16.5, 9.4, 6.2 Hz, 2H), 1.67–1.63 (m, 2H), 1.49–1.47 (m, 2H), 1.34 (t, J = 7.1 Hz, 1H). ^{13}C NMR (101 MHz, Methanol-d_4) δ 142.5 (d, J = 3.2 Hz), 128.1–127.9 (m), 125.2, 41.3 (d, J = 134.8 Hz), 35.3, 31.5–31.4 (m), 26.9–26.9 (m), 23.3. ^{31}P NMR (162 MHz, Methanol-d_4) δ 30.5. HRMS (ESI): Calcd. for $C_{12}H_{19}O_3NaPS$ [M+H]$^+$ 297.0690; found 297.0685.

4.1.7. General procedure for the synthesis of acrylonitriles (13a and 13b)

Compound **13a** and **13b** were prepared by a modified procedure based on the work of Baraldi et al. [39] K_2CO_3 (3 equiv) and 4-cyano-3-oxotetrahydrothiophene **12** (1 equiv) were stirred in dry acetone (20 mL). To this suspension alkyl halide (1 equiv) was added and the mixture was refluxed for 5 h. The residue was dissolved in ether and stirred vigorously with 5% NaOH aq. (10 mL). The solution was kept at RT until complete fragmentation of the intermediate adduct was observed by TLC. The organic phase was separated and dried with sodium sulfate. The crude oil was further purified by column chromatography using 20% diethyl ether in pentane as eluent.

4.1.7.1. 2-Benzylacrylonitrile (13a). K_2CO_3 (11.7 mmol, 1.62 g, 3 equiv), compound 4-cyano-3-oxotetrahydrothiophene (3.9 mmol, 0.5 g, 1 equiv), and benzyl bromide (3.9 mmol, 0.673 g, 1 equiv), gave **13a** as an oil (1.99 mmol, 284 mg, 51%). ^{1}H NMR (400 MHz, Chloroform-d) δ 7.40 (t, J = 8.0 Hz, 2H), 7.33 (d, J = 7.3 Hz, 1H), 7.26 (d, J = 7.4 Hz, 2H), 5.95 (s, 1H), 5.73 (s, 1H), 3.59 (s, 2H). ^{13}C NMR (101 MHz, Chloroform-d) δ 135.6, 131.1, 129.2, 128.9, 128.9, 128.6, 128.6, 128.4, 127.4, 122.7, 118.5, 40.8. HRMS (ESI): Calcd. for $C_{10}H_{10}N$ [M+H]$^+$ 144.0808; found 144.0808.

4.1.7.2. 2-Methylene-5-phenylpentanenitrile (13b).

K_2CO_3 (47.1 mmol, 6.51 g, 3 equiv), 4-cyano-3-oxotetrahydrothiophene (15.7 mmol, 2.00 g, 1 equiv), 1-bromo-3-phenylpropane (15.7 mmol, 3.13 g, 1 equiv), gave 13b as an oil (3.29 mmol, 564 mg, 21%). ^{1}H NMR (400 MHz, Chloroform-d) δ 7.34 (dd, J = 8.1, 6.7 Hz, 2H), 7.24–7.19 (m, 3H), 5.87 (s, 1H), 5.71 (d, J = 1.6 Hz, 1H), 2.68 (t, J = 7.6 Hz, 2H), 2.29–2.27 (m, 2H), 1.96–1.90 (m, 2H),. ^{13}C NMR (101 MHz, Chloroform-d) δ 141.1, 130.5, 128.5, 128.5, 128.4, 126.1, 122.9, 118.6, 34.7, 33.9, 29.1. HRMS (ESI): Calcd. for $C_{12}H_{14}N_4$ $[M+H]^+$ 172.1114; found 172.1121.

4.1.8. General procedure for the preparation of tetrazoles (14a and 14b)

Dibutyltin oxide (0.2 equiv) and trimethylsilyl azide (2 equiv) were added to a solution of 13 (1 equiv) in anhydrous 1,4-dioxane (2 mL/mmol). The reaction mixture was subjected to microwave irradiation in a tightly sealed vessel for 50 min at 150 °C, then cooled to room temperature. The solvent was removed under reduced pressure. The residue was dissolved in diethyl ether (10 mL and extracted with 2 M aq. NaOH (3 × 10 mL). The aqueous layer was acidified with 4 M aq. HCl to pH 1 and extracted with ethyl acetate (4 × 10 mL). The organic extract was washed with brine (10 mL), dried over MgSO4, and evaporated under reduced pressure to give the target tetrazoles, which were recrystallized from EtOAc.

4.1.8.1. 5-(3-Phenylprop-1-en-2-yl)-1H-tetrazole (14a).

Dibutyltin oxide (0.07 mmol, 0.017 g, 0.2 equiv), trimethylsilyl azide (1.4 mmol, 0.161 g, 2 equiv) and 13a (0.100 g, 0.7 mmol, 1 equiv) gave 14a (0.55 mmol, 102 mg, 78%). ^{1}H NMR (400 MHz, Methanol-d_4) δ 7.35–7.18 (m, 5H), 6.04 (s, 1H), 5.47 (s, 1H), 4.92 (s, 1H), 3.92 (s, 2H). ^{13}C NMR (101 MHz, Methanol-d_4) δ 137.5, 133.2, 128.7, 128.1, 126.3, 120.3, 38.9. HRMS (ESI): Calcd. for $C_{10}H_{10}N_4$ $[M+H]^+$ 187.0981; found 187.0978.

4.1.8.2. 5-(5-Phenylpent-1-en-2-yl)-1H-tetrazole (14b).

Dibutyltin oxide (0.58 mmol, 145.39 mg, 0.2 equiv), trimethylsilyl azide (5.84 mmol, 0.672 g, 2 equiv) and 13b (2.92 mmol, 1 equiv) gave 14b (2.16 mmol, 462 mg, 74%). ^{1}H NMR (400 MHz, Chloroform-d) δ 7.14–7.00 (m, 5H), 5.87 (s, 1H), 5.47 (t, J = 1.4 Hz, 1H), 4.84–4.83 (m, 1H), 2.58 (dd, J = 15.7, 7.8 Hz, 4H), 1.78 (m, 2H). ^{13}C NMR (101 MHz, Chloroform-d) δ 157.3, 143.1, 134.7, 129.4, 129.4, 126.9, 120.6, 36.2, 34.0, 30.9. HRMS (ESI): Calcd. for $C_{12}H_{15}N_4$ $[M+H]^+$ 215.1292; found 215.1291.

4.1.9. General procedure for the Michael addition to vinylic tetrazoles (preparation of 15 and 16)

Vinylic tetrazole 14 (1 equiv) and thioacetic acid (26 equiv) or thiol (4 equiv) were dissolved in anhydrous DMF. The reaction mixture was subjected to heating at 60 °C in a tightly sealed vessel for 22 h with stirring. The solvent was removed under reduced pressure and the crude was subjected to column chromatography using 5% MeOH in CH_2Cl_2.

4.1.9.1. S-(3-phenyl-2-(1H-tetrazol-5-yl)propyl) ethanethioate (15a).

14a (0.32 mmol, 0.060 g, 1 equiv), and thioacetic acid (8.6 mmol, 0.662 g, 26 equiv) gave 15a (0.30 mmol, 79 mg, 95%) as a colorless oil. ^{1}H NMR (400 MHz, Chloroform-d) δ 7.20–7.16 (m, 3H), 7.08–7.06 (m, 2H), 3.86 (q, J = 10.5, 7.7 Hz, 1H), 3.44–3.40 (m, 1H), 3.33 (d, J = 14.0 Hz, 1H), 3.23 (d, J = 7.6 Hz, 2H), 2.27 (s, 3H). ^{13}C NMR (101 MHz, Chloroform-d) δ 195.9, 157.9, 137.0, 128.9, 128.9, 128.7, 127.0, 39.7, 38.0, 31.8, 30.6. HRMS (ESI): Calcd. for $C_{12}H_{15}ON_4S$ $[M+H]^+$ 263.0964; found 263.0961.

4.1.9.2. S-(5-phenyl-2-(1H-tetrazol-5-yl)pentyl) ethanethioate (15b).

14b (0.466 mmol, 0.100 mg, 1 equiv), and thioacetic acid (12.1 mmol, 0.925 g, 26 equiv) gave 15b (0.456 mmol, 132 mg, 98%) as a colorless oil. ^{1}H NMR (400 MHz, Methanol-d_4) δ 7.22–7.11 (m, 5H), 4.93 (s, 1H), 3.38–3.30 (m, 2H), 3.16 (dd, J = 15.2, 10.3 Hz, 1H), 2.58 (t, J = 7.5 Hz, 2H), 2.24 (s, 3H), 1.91–1.77 (m, 2H), 1.61–1.45 (m, 2H). ^{13}C NMR (101 MHz, Methanol-d_4) δ 196.2, 159.6, 142.9, 129.4, 126.9, 37.2, 36.2, 33.9, 33.3, 30.4, 29.9. HRMS (ESI): Calcd. for $C_{14}H_{19}ON_4S$ $[M+H]^+$ 291.1284; found 291.1274.

4.1.9.3. ′5-(1-(cyclohexylthio)-5-phenylpentan-2-yl)-1H-tetrazole (16).

14a (0.23 mmol, 0.050 g, 1 equiv), and cyclohexyl thiol (0.933 mmol, 0.108 g, 4 equiv) gave 16 (0.216 mmol, 71.50 mg, 93%). ^{1}H NMR (400 MHz, Methanol-d_4) δ 7.23–7.09 (m, 5H), 2.95–2.82 (m, 1H), 2.58–2.55 (m, 2H), 1.86–1.68 (m, 6H), 1.59–1.18 (m, 10H). ^{13}C NMR (101 MHz, Methanol-d_4) δ 158.94, 141.6, 127.9, 127.9, 125.5, 43.6, 36.7, 34.9, 33.6, 33.4, 33.3, 32.8, 28.6, 25.6, 25.5. HRMS (ESI): Calcd. for $C_{18}H_{27}N_4S$ $[M+H]^+$ 331.1950; found 331.1951.

4.2. Biological activity

4.2.1. Gene constructs of VIM-2, NDM-1 and GIM-1

In this study two types of gene constructs were used. The first included the native leader sequence to allow the proteins to be transported to the periplasm, for the three enzymes VIM-2 from *Pseudomonas aeruginosa strain 301-5473* (GenBank no Q9K2N0 [51]), GIM-1 from *P. aeruginosa* (GenBank no Q704V1 [50,52]) and NDM-1 (GenBank no. E9NWK5, e.g. refs. [53,54]), where the latter bla_{NDM-1} gene is reported from several organisms. Cloning of bla_{NDM-1} or bla_{GIM-1} genes into the *Escherichia coli* pET26b(+) vector (Novagen) was performed using the Primers listed in Table S3, and by restriction cutting as described for VIM-26 [55]. Cloning of bla_{VIM-2} into pET26b(+)are described previously [56]. The obtained *E. coli* pET-26b(+) MBL constructs were further used in the in the whole cell-based inhibitor assays.

In the second gene constructs used for the recombinant gene expression, the native leader sequence was removed and replaced with a hexa-His tag and a TEV cleavage site as reported earlier for VIM-2 (residues V27-E268 [51]) and GIM-1 (residues Q19-D250 [50]) both in pDEST14. NDM-1 used a codon optimized synthetic gene (Life Technologies, Thermo Fisher Scientific), with a TEV cleavage site with sequence ENLYFQG and residues G36-R280 in NDM-1 transformed in pDONR™221, and further sub cloned into pDEST17 with carries an N-terminal hexa His-tag, yielding pDest17-NDM-1. Herein the residue numbering is the class B β-lactamase numbering scheme will be applied [10].

4.2.2. Recombinant protein expression and purification of VIM-2, GIM-1 and NDM-1

The three proteins were expressed and purified following this protocol. pDest17-NDM-1 was transformed into *E. coli* BL21 Star (DE3) pLysS (Invitrogen), and pDEST14 plasmids with VIM-2 or GIM-1 were transformed into in-house modified *E. coli* BL21 Star (DE3) pLysS (Invitrogen) cells with the pRARE plasmid (Novagen) in order to allow expression of genes encoding tRNAs for rare codons [57]. Precultures grown in Terrific Broth (TB) media with 100 μg/mL ampicillin (Sigma-Aldrich) and 34 μg/mL chloramphenicol (Sigma-Aldrich). The precultures were inoculated to 2 L Luria-Bertani (LB) media containing 100 μg/mL ampicillin and 34 μg/mL chloramphenicol and grown at 37 °C to reach an optical density (OD$_{600}$ nm) of 0.5–1.0 before induced expression with 0.4 mM isopropyl β-D-1-thigalactopyranoside (IPTG; Sigma-Aldrich). The induced cultures were grown overnight at 20 °C before collecting the cells by centrifugation (8900 × g, 30 min, 4 °C). Buffer A containing 50 mM HEPES pH 7.2, 100 μM $ZnCl_2$ and 150 mM NaCl was used to resuspend the cell pellets, following sonication and collecting the supernatants by centrifugation (3000 g, 40 min, 4 °C). The

recombinant proteins were affinity purified using a 1 mL or 5 mL His-Trap HP column (GE Healthcare) in buffer A washed with 5% buffer B (50 mM HEPES pH 7.2, 100 μM ZnCl$_2$, 150 mM NaCl and 1 M imidazole), before eluted in a gradient of 5–100% buffer B. Peak fractions were investigated using 4–20% sodium dodecyl sulfate polyacrylamide gel electrophoresis (SDS-PAGE; Bio-Rad) [58]. The peaks containing MBL protein was added in-house-made His-tagged TEV protease in a 1:100 mg ratio of TEV:protein and dialyzed at 4 °C overnight using 10-kDa cutoff Snakeskin (Pierce) in buffer C (50 mM HEPES pH 7.2, 150 mM NaCl, 1 mM EDTA and 1 mM β-mercaptoethanol). To remove uncleaved protein and TEV protease a second His-Trap purification was performed. SDS-PAGE analysis was used to estimate a purity of ~95% of the fractions containing protein, which then were pooled and dialyzed in buffer A overnight.

4.2.3. Co-crystallization of VIM-2 with **2b**, **10b** and **10c**

Co-crystallization of VIM-2 was successful with inhibitors **2b**, **10b** and **10c**, when applying our new protocol for DMSO free co-crystallization [45]. MRC 96-wells were pre-coated with 3 μl inhibitor (100 mM) dissolved in DMSO, and DMSO evaporated after leaving the plates in the fume hood for 24 h 60 μL reservoir solution consisting of 22–27% PEG 3350 and 0.2 M magnesium formate was added to each well. The crystallization plates were then shaken for 24 h to allow the inhibitors to dissolve, followed by manual mixing of hanging drops in a 1:1 ratio of VIM-2 (9.4 mg/mL) and reservoir. The crystals were cryoproceeded in 25% PEG 3350, 0.2 M MgCl$_2$, 15% ethylene glycol and 50 mM HEPRS pH 7.2, before they were flash cooled in liquid nitrogen and X-ray data collected at ESRF, ID29.

Coordinate and structure factor files for the VIM-2_**2b** (PDB accession number 5MM9), VIM-2_**10b** (PDB accession number 5NHZ) and VIM-2_**10c** (PDB accession number 5NI0) were deposited in the Protein Data Bank (PDB).

4.2.4. Dose rate inhibition studies for IC$_{50}$ determination

The half-maximal inhibitory concentration (IC$_{50}$) against the VIM-2, NDM-1 and GIM-1 enzymes were determined by using sixteen different concentration of inhibitor compounds ranging from 0 μM to 250 μM. A 100 μl solution with 50 mM HEPES buffer (pH 7.2), 100 μM ZnCl$_2$, purified enzyme (10 nM VIM-2, NDM-1 or GIM-1) and 2.5–0 mM inhibitor were incubated in a 96 well plate at 25 °C for 5 min. In addition, the enzyme buffer contained 400 μg/mL Bovine Serum Albumin (BSA) to prevent protein unfolding and loss of activity due to low concentrations [59,60]. 100 μM of the reporter substrate nitrocefin (VIM-2, GIM-1) or imipenem (NDM-1) was added to the enzyme-inhibitor solution and the increase in absorbance at 482 nm (nitrocefin) or 260 nm (imipenem) was recorded on a Spectramax M2e spectrophotometer (Molecular Devices). Each data point was performed in triplicates and the initial velocity for each inhibitor concentration was analyzed by a log [inhibitor] vs. response curve fitting to calculate IC$_{50}$ in GraphPad Prism 5.0 software.

4.2.5. Cell-based screening assay of the inhibition potential

The inhibitory activity of the inhibitors was investigated in a cell-based assay using a β-lactamase-negative *E. coli* SNO3 (*ampA1 ampC8 pyrB recA rpsL*) (24) transformed with pET26b(+) containing *bla*$_{VIM-2}$, *bla*$_{GIM-1}$ or *bla*$_{NDM-1}$. The screen was conducted in 96-well plates (Corning) in duplicates. One μl inhibitor (final concentration 250 μM), 50 μl overnight culture (adjusted to an OD$_{600}$ of 1 in LB broth) of *E. coli* SNO3 containing one of the MBLs and 50 μl LB media with final concentration 0.8 mM Isopropyl ß-D-1-thiogalactopyranoside (Sigma, IPTG) was added to each well. The plate was incubated at 37 °C for 20 min with shaking to induce the expression of the MBL. Subsequently, 50 μl nitrocefin (diluted in 50 mM HEPES pH 7.2 and 100 μM ZnCl$_2$ to give a final concentration

of 1.6 mM in the assay) was added. Nitrocefin hydrolysis was measured at OD$_{482}$ every minute for 3 h with shaking (47 s) in between reads using a Spectramax M2^e spectrophotometer (Molecular Devices). EDTA (250 μM concentration) was used as positive control and wells containing no inhibitor as negative controls. The percent inhibition was calculated according to equation (1).

$$\% \text{ inhibition} = \left(\frac{\text{Slope}_{(\text{No inhibitor})} - \text{Slope}_{(\text{Inhibitor})}}{\text{Slope}_{(\text{No inhibitor})}} \right) \times 100 \%$$

(1)

The synergistic effect of the inhibitors with meropenem was tested against selected clinical bacterial strains containing MBLs. The bacterial strains were plated on lactose agar plates with 100 mg/L ampicillin and lactose agar and incubated overnight at 37 °C. The inhibitors were diluted to a final concentration of 125 μM in Mueller Hinton (MH) broth. In order to monitor the effect of the DMSO in the assay, a DMSO control was included with a concentration of 5%. Meropenem was diluted in MH broth in a 2-fold dilution series with final concentrations of 256 μg/mL − 0.0625 μg/mL. The microtiter plates were inoculated with a 0.5 McFarland suspension of the bacterial strain in 0.85% NaCl, which were diluted in MH broth. A quality check of bacterial suspension in 0.85% NaCl in a 1:100 ratio was incubated on MH agar plates overnight at 37 °C. The final CFU/mL inoculum was calculated and compared to a standard. The microtiter plates were incubated for 20 h at 37 °C. The minimum inhibitory concentrations (MIC) were read visually of the plates the next day.

Acknowledgments

Appendix A. Supplementary data

Supplementary data related to this article can be found at http://dx.doi.org/10.1016/j.ejmech.2017.04.035.

References

[1] World Health Organization (WHO), Antimicrobial Resistance: Global Report on Surveillance, 2014.
[2] World Health Organization (WHO), The Evolving Threat of Antimicrobial Resistance : Options for Action, 2012.
[3] A.M. Queenan, K. Bush, Clin. Microbiol. Rev. 20 (2007) 440–458.
[4] J.D. Pitout, Drugs 70 (2010) 313–333.
[5] R.P. Ambler, Philos. Trans. R. Soc. B 289 (1980) 321–331.
[6] K. Bush, G.A. Jacoby, Antimicrob. Agents Chemother. 54 (2010) 969–976.
[7] T.R. Walsh, Int. J. Antimicrob. Agents 36 (2010) S8–S14.
[8] T. Palzkill, Ann. N. Y. Acad. Sci. 1277 (2013) 91–104.
[9] J. Jeon, J. Lee, J. Lee, K. Park, A. Karim, C.-R. Lee, B. Jeong, S. Lee, Int. J. Mol. Sci. 16 (2015) 9654–9692.
[10] G. Garau, I. García-Sáez, C. Bebrone, C. Anne, P. Mercuri, M. Galleni, J.M. Frère, O. Dideberg, Antimicrob. Agents Chemother. 48 (2004) 2347–2349.
[11] T.R. Walsh, M.A. Toleman, L. Poirel, P. Nordmann, Clin. Microbiol. Rev. 18 (2005) 306–325.
[12] G. Patel, R. Bonomo, Front. Microbiol. 4 (2013) 1–17.
[13] J.D. Buynak, Biochem. Pharmacol. 71 (2006) 930–940.
[14] J.L. Liscio, M.V. Mahoney, E.B. Hirsch, Int. J. Antimicrob. Agents 46 (2015) 266–271.
[15] S.M. Drawz, K.M. Papp-Wallace, R.A. Bonomo, Antimicrob. Agents Chemother. 58 (2014) 1835–1846.
[16] M.M. González, A.J. Vila, in, Springer Berlin Heidelberg, Berlin, Heidelberg, 2016, pp. 1–34.
[17] W. Jing-Fang, C. Kuo-Chen, Curr. Top. Med. Chem. 13 (2013) 1242–1253.
[18] W. Fast, L.D. Sutton, Biochim. Biophys. Acta (2013) 1648–1659.

[19] J. Brem, S.S. van Berkel, D. Zollman, S.Y. Lee, O. Gileadi, P.J. McHugh, T.R. Walsh, M.A. McDonough, C.J. Schofield, Antimicrob. Agents Chemother. 60 (2016) 142–150.
[20] F.-M. Klingler, T.A. Wichelhaus, D. Frank, J. Cuesta-Bernal, J. El-Delik, H.F. Müller, H. Sjuts, S. Göttig, A. Koenigs, K.M. Pos, D. Pogoryelov, E. Proschak, J. Med. Chem. 58 (2015) 3626–3630.
[21] M.M. González, M. Kosmopoulou, M.F. Mojica, V. Castillo, P. Hinchliffe, I. Pettinati, J. Brem, C.J. Schofield, G. Mahler, R.A. Bonomo, L.I. Llarrull, J. Spencer, A.J. Vila, ACS Infect. Dis. 1 (2015) 544–554.
[22] N. Li, Y. Xu, Q. Xia, C. Bai, T. Wang, L. Wang, D. He, N. Xie, L. Li, J. Wang, H.-G. Zhou, F. Xu, C. Yang, Q. Zhang, Z. Yin, Y. Guo, Y. Chen, Bioorg. Med. Chem. Lett. 24 (2014) 386–389.
[23] B.M.R. Liénard, G. Garau, L. Horsfall, A.I. Karsisiotis, C. Damblon, P. Lassaux, C. Papamicael, G.C.K. Roberts, M. Galleni, O. Dideberg, J.M. Frère, C.J. Schofield, Org. Biomol. Chem. 6 (2008) 2282–2294.
[24] Q. Sun, A. Law, M.W. Crowder, H.M. Geysen, Bioorg. Med. Chem. Lett. 16 (2006) 5169–5175.
[25] W.C. Jin, Y. Arakawa, H. Yasuzawa, T. Taki, R. Hashiguchi, K. Mitsutani, A. Shoga, F. Xu, Y. Yamaguchi, H. Kurosaki, N. Shibata, M. Ohta, M. Goto, Biol. Pharm. Bull. 27 (2004) 851–856.
[26] U. Heinz, R. Bauer, S. Wommer, W. Meyer-Klaucke, C. Papamichaels, J. Bateson, H.W. Adolph, J. Biol. Chem. 278 (2003) 20659–20666.
[27] C. Mollard, C. Moali, C. Papamicael, C. Damblon, S. Vessilier, G. Amicosante, C.J. Schofield, M. Galleni, J.-M. Frère, G.C.K. Roberts, J. Biol. Chem. 276 (2001) 45015–45023.
[28] N.O. Concha, C.A. Janson, P. Rowling, S. Pearson, C.A. Cheever, B.P. Clarke, C. Lewis, M. Galleni, J.-M. Frère, D.J. Payne, J.H. Bateson, S.S. Abdel-Meguid, Biochemistry-US 39 (2000) 4288–4298.
[29] M.I. Page, A.P. Laws, Chem. Commun. (1998) 1609–1617.
[30] S. Bounaga, A.P. Laws, M. Galleni, M.I. Page, Biochem. J. 331 (1998) 703–711.
[31] M. Goto, T. Takahashi, F. Yamashita, A. Koreeda, H. Mori, M. Ohta, Y. Arakawa, Biol. Pharm. Bull. 20 (1997) 1136–1140.
[32] J. Brem, S.S. van Berkel, W. Aik, A.M. Rydzik, M.B. Avison, I. Pettinati, K.-D. Umland, A. Kawamura, J. Spencer, T.D.W. Claridge, M.A. McDonough, C.J. Schofield, Nat. Chem. 6 (2014) 1084–1090.
[33] G.A. Patani, E.J. LaVoie, Chem. Rev. 96 (1996) 3147–3176.
[34] C. Ballatore, D.M. Huryn, A.B. Smith, ChemMedChem 8 (2013) 385–395.
[35] Y. Yamaguchi, W. Jin, K. Matsunaga, S. Ikemizu, Y. Yamagata, J.I. Wachino, N. Shibata, Y. Arakawa, H. Kurosaki, J. Med. Chem. 50 (2007) 6647–6653.
[36] J.D. Park, D.H. Kim, J. Med. Chem. 45 (2002) 911–918.
[37] R.V. Bikbulatov, F. Yan, B.L. Roth, J.K. Zjawiony, Bioorg. Med. Chem. Lett. 17 (2007) 2229–2232.
[38] L. Zervas, I. Photaki, N. Ghelis, J. Am. Chem. Soc. 85 (1963) 1337–1341.
[39] P.G. Baraldi, G.P. Pollini, V. Zanirato, A. Barco, S. Benetti, Synthesis (1985) 969–970.
[40] S.M. Lukyanov, I.V. Bliznets, S.V. Shorshnev, G.G. Aleksandrov, A.E. Stepanov, A.A. Vasil'ev, Tetrahedron 62 (2006) 1849–1863.
[41] T. Christopeit, H.K. Leiros, Bioorg. Med. Chem. Lett. 26 (2016) 1973–1977.
[42] S. Skagseth, T.J. Carlsen, G.E. Bjerga, J. Spencer, Ø. Samuelsen, H.K.S. Leiros, Antimicrob. Agents Chemother. 60 (2015) 990–1002.
[43] P. Lassaux, M. Hamel, M. Gulea, H. Delbrück, P.S. Mercuri, L. Horsfall, D. Dehareng, M. Kupper, J.M. Frère, K. Hoffmann, M. Galleni, C. Bebrone, J. Med. Chem. 53 (2010) 4862–4876.
[44] H. Nikaido, Microbiol. Mol. Biol. Rev. 67 (2003) 593–656.
[45] T. Christopeit, K.-W. Yang, S.-K. Yang, H.-K.S. Leiros, Acta Cryst. F72 (2016) 813–819.
[46] H. Kurosaki, Y. Yamaguchi, H. Yasuzawa, W.C. Jin, Y. Yamagata, Y. Arakawa, ChemMedChem 1 (2006) 969–972.
[47] P. Hinchliffe, M.M. González, M.F. Mojica, J.M. González, V. Castillo, C. Saiz, M. Kosmopoulou, C.L. Tooke, L.I. Llarrull, G. Mahler, R.A. Bonomo, A.J. Vila, J. Spencer, Proc. Natl. Acad. Sci. U. S. A. 113 (2016) E3745–E3754.
[48] M.F. Mojica, S.G. Mahler, C.R. Bethel, M.A. Taracila, M. Kosmopoulou, K.M. Papp-Wallace, L.I. Llarrull, B.M. Wilson, S.H. Marshall, C.J. Wallace, M.V. Villegas, M.E. Harris, A.J. Vila, J. Spencer, R.A. Bonomo, Biochemistry-US 54 (2015) 3183–3196.
[49] D.T. King, L.J. Worrall, R. Gruninger, N.C.J. Strynadka, J. Am. Chem. Soc. 134 (2012) 11362–11365.
[50] P.S. Borra, Ø. Samuelsen, J. Spencer, T.R. Walsh, M.S. Lorentzen, H.-K.S. Leiros, Antimicrob. Agents Chemother. 57 (2013) 848–854.
[51] T. Christopeit, T.J. Carlsen, R. Helland, H.-K.S. Leiros, J. Med. Chem. (2015) 8671–8682.
[52] M. Castanheira, M.A. Toleman, R.N. Jones, F.J. Schmidt, T.R. Walsh, Antimicrob. Agents Chemother. 48 (2004) 4654–4661.
[53] D. Yong, M.A. Toleman, C.G. Giske, H.S. Cho, K. Sundman, K. Lee, T.R. Walsh, Antimicrob. Agents Chemother. 53 (2009) 5046–5054.
[54] K.K. Kumarasamy, M.A. Toleman, T.R. Walsh, J. Bagaria, F. Butt, R. Balakrishnan, U. Chaudhary, M. Doumith, C.G. Giske, S. Irfan, P. Krishnan, A.V. Kumar, S. Maharjan, S. Mushtaq, T. Noorie, D.L. Paterson, A. Pearson, C. Perry, R. Pike, B. Rao, U. Ray, J.B. Sarma, M. Sharma, E. Sheridan, M.A. Thirunarayan, J. Turton, S. Upadhyay, M. Warner, W. Welfare, D.M. Livermore, N. Woodford, Lancet Infect. Dis. 10 (2010) 597–602.
[55] H.-K.S. Leiros, K.S.W. Edvardsen, G.E.K. Bjerga, Ø. Samuelsen, FEBS J. 282 (2015) 1031–1042.
[56] Ø. Samuelsen, M. Castanheira, T.R. Walsh, J. Spencer, Antimicrob. Agents Chemother. 52 (2008) 2905–2908.
[57] E.A. Rogulin, T.A. Perevyazova, L.A. Zheleznaya, N.I. Matvienko, Biochemistry-Moscow+ 69 (2004) 1123–1127.
[58] U.K. Laemmli, Nature 227 (1970) 680–685.
[59] N. Laraki, N. Franceschini, G.M. Rossolini, P. Santucci, C. Meunier, E. de Pauw, G. Amicosante, J.M. Frère, M. Galleni, Antimicrob. Agents Chemother. 43 (1999) 902–906.
[60] S. Siemann, D.P. Evanoff, L. Marrone, A.J. Clarke, T. Viswanatha, G.I. Dmitrienko, Antimicrob. Agents Chemother. 46 (2002) 2450–2457.